# Earth & Space Sciences Publication Highlights

**Research on volcanic activity in the Yucca Mountain area published**

EES Division members working to assess volcanic risk for the proposed Yucca Mountain radioactive waste repository recently published a paper that describes in detail the Lathrop Wells scoria cone volcano—the most important analog to potential future activity in the Yucca Mountain region (Valentine GA, Krier DJ, Perry FV, Heiken G, 2007, "Eruptive and geomorphic processes at the Lathrop Wells scoria cone volcano," ***Journal of Volcanology and Geothermal Research***, v. 161, pp. 57-80 (2007). The authors show that that the volcano is monogenetic (erupted in one episode lasting months to a few years), in contrast to previous theories of the volcano having polycyclic activity. A wide range of eruptive processes occurred with little change in major element composition. The researchers conclude that the variation in explosive and effusive processes, including their simultaneous occurrence; must result entirely from fluid dynamic, crystallization, and degassing process in the ascending multiphase magma. The study is of interest to the Yucca Mountain Project because it helps define parameters for risk assessment, and to the broader volcanology community because of the growing interest in basaltic eruptive processes.

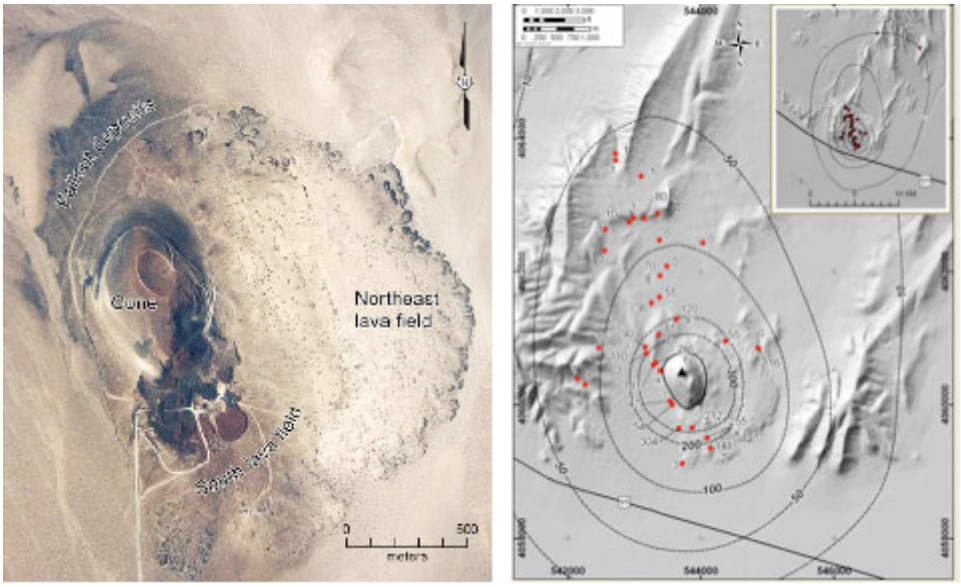


*Figure Left: aerial photograph of the Lathrop Wells volcano. Right: Contours of thickness of fallout deposits from the eruption, units in cm. Inset shows possible regional extent based upon thin (~1 cm) remnants of ash in distal locations. Lettered stations refer to stratigraphic columns.*

**Imaging fractures applying Time Reversal Nonlinear Elastic Wave Spectroscopy (NEWS) published**

T. J. Ulrich, Paul Johnson, and Robert Guyer (all in EES-11) published laboratory imaging results on the interaction of cracks with elastic waves in the March 9th, 2007, issue of ***Physical Review Letters***(URL: http://link.aps.org/abstract/PRL/v98/e104301). The acoustics group in EES is developing crack ("damage") imaging methods that combine Nonlinear Non-Destructive Evaluation (NDE) [also termed Nonlinear Elastic Wave Spectroscopy, NEWS] and time reverse acoustics. The general method is termed Time Reversal Nonlinear Elastic Wave Spectroscopy (TR NEWS). The basis of the method is to excite two waves in a solid. If a crack is present, *nonlinear mixing results at the crack*, and sidebands (sum and difference frequency waves) are formed. Other scatterers, such as layer boundaries, voids etc. *produce only linear scattering*. The

full signal train is detected, and one filters out all but the sidebands. Following this, one time-reverses the filtered signal, re-emits it from the detector, and it focuses at the nonlinear source, *i.e.*, the crack. An example of a TR NEWS imaging experiment is shown in the figure. In the case of internal cracks in a 3-D solid, one cannot detect at the location of a fracture. Thus a modified method is used, whereby the detected signal is filtered and time reversed, but the wave is back propagated through a velocity model. Therefore the crack can be located if the velocity model is good. Efforts are being made to apply very similar methods for earthquake source localization and to study source complexity. LDRD supported the research. For more information: http://www.lanl.gov/orgs/ees/ ees11/geophysics/nonlinear/nonlinear.shtml

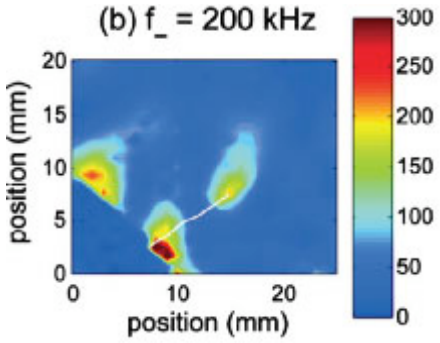


*Figure: The crack is shown as a thin white line. The hot spots are associated with the crack opening and crack tip. A secondary hot spot is believed to be due to geometrical scattering of the sideband wave.*

**Publications in *Plant, Cell and Environment* on climate change impacts on ecosystem**

Two new publications in ***Plant, Cell and Environment*** highlight innovative techniques being developed and tested by Nate McDowell and his team in the Atmospheric, Climate and Environmental Dynamics Group (EES-2). Tunable Diode Laser (TDL) techniques, refined and improved by the team, have allowed the first continuous, high precision and high frequency isotopic $CO_2$ flux measurements at the tissue scale. These two papers are the first to demonstrate that TDL's can be applied to tissue level analyses (*e.g.* foliar isotope fluxes). This significant advancement allowed the researchers to discover new insights in foliar carbon metabolism and foliar water/$CO_2$ interactions. They are now pushing the TDL technique towards long-term monitoring of climate change impacts on carbon and water fluxes at ecosystem scales. The EES-2 team has the only long-term (3 years) data set of continuous measurements exchanged between a terrestrial ecosystem and the atmosphere; this unique data set is shedding novel insights into how climate impacts ecosystem metabolism. The 3-year data set on ecosystem isotopic fluxes is the subject of a workshop on measurement and model comparisons, funded by IGPP and hosted by EES-2, March 28-30, 2007 in Santa Fe. This new method of continuous measurement is being adopted by the National Science Foundation as an early warning system of ecological collapse.

*Figure: An open leaf gas exchange system coupled to a tunable diode laser (TDL) allowed measurement of the isotope composition of leaf-respired $CO_2$ online and in real time.*

**Groundbreaking results published in the *Journal of Geophysical Research***

Researchers Donatella Pasqualini (EES-9), Katrin Heitmann (ISR-1), James TenCate (EES-11), Salman Habib (T-08), David Higdon (CCS-6), and Paul A. Johnson (EES-11) have investigated the nonlinear elastic properties of rocks at amplitudes lower than have ever been explored in order to understand the onset of elastic nonlinearity. The collaborators studied Berea and Fontainebleau sandstones, and characterized their behavior by applying resonant-bar experiments under carefully controlled thermal and humidity conditions. This study establishes the existence of two strain regimes: 1) where the material shows classical nonlinearity (this has never before been characterized), and 2) where the behavior becomes truly nonequilibrium—as demonstrated by the existence of relaxation (slow dynamics)—and where the theory of classical nonlinearity no longer applies. The separate effects of nonlinearity and relaxation in this regime cannot be disentangled.

This transition from classical nonlinearity to nonlinear nonequilibrium dynamics elasticity in rocks is of significance in understanding the basic dynamical processes in consolidated granular materials. The new experimental evidence and the theoretical interpretation present a breakthrough for the investigation of the nonlinear elastic behavior of geomaterials, underscoring the need for new experiments and a new theoretical framework. The researchers described the preliminary results in a previous paper in ***Physical Review Letters***, 93, 06551-06555 (2004). The most recent results have been published in "Nonequilibrium and nonlinear dynamics in Berea and Fontainebleau sandstones: Low-strain regime," ***J. Geophys. Res.,*** Vol. 112, No. B1, B01204 10.1029/2006JB004264 (2007). The research was funded in part through the DOE Office of Basic Energy Science and the Institute of Geophysics and Planetary Physics (IGPP) at LANL.

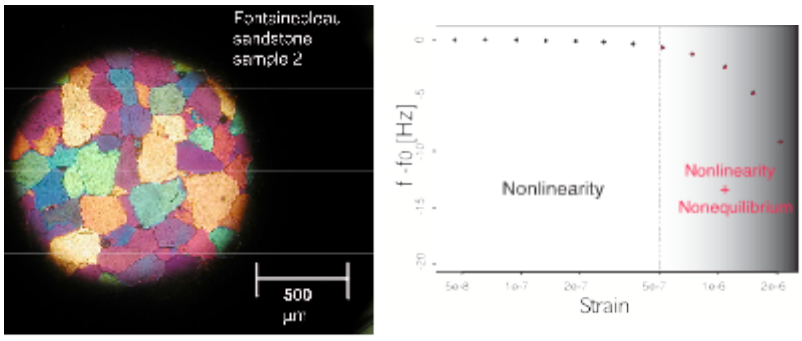


*Figure: (a) Polarized thin section of Fontainebleau, one of the two rocks studied in this paper. Figure (b) Resonance frequency (linked to the elastic modulus) shift versus strain. For strains below 5*10-7, the material displays only an intrinsic reversible nonlinearity; for strains above 5*10-7,nonlinear and nonequilibrium effects are combined.*

**EES scientists author invited review book chapters**

Paul Johnson, Jim TenCate, Michele Griffa, Thomas Shankland (all EES-11); Donetella Pasqualini (EES-9); and Palo Patelli (EES-2) have written invited review chapters in the recently published book, ***Universality of Nonclassical Nonlinearity***, Applications to Non-Destructive Evaluations and Ultrasonics, Delsanto, (Pier Paolo, Ed.), 2007. The book chapters including LANL authors are the following:

- J. A.Tencate, T. J. Shankland, and P. A. Johnson, "Nonlinear Elastic Wave Experiments: Learning About the Behaviour of Rocks and Geomaterials"
- P. A. Johnson, "Nonequilibrium Nonlinear Dynamics in Solids State of the Art"
- Paolo Patelli, "Nonlinear Dynamical Systems in Economics"

- Donatella Pasqualini, “Intrinsic Nonlinearity in Geomaterials: Elastic Properties of Rocks at Low Strain”
- Silvia Delsanto, Michele Griffa, and Lia Morra, “Inverse Problems and Genetic Algorithms”

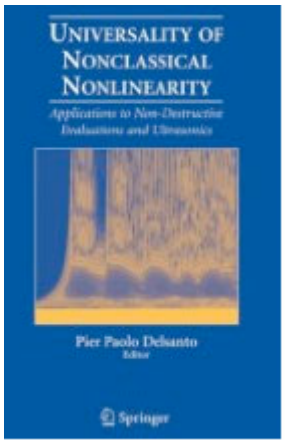


This book is a result of research developed in the framework of two large international projects: 1) the European Science Foundation (ESF) supported program NATEMIS (Nonlinear Acoustic Techniques for Micro-Scale Damage Diagnostics) and 2) a LANL-based network headed by Paul A. Johnson (EES-11). The main topic of both programs and of this book is the description of the phenomenology, theory and applications of Nonclassical Nonlinearity (NCNL). The NCNL techniques have been found to be extremely powerful (up to more than 1000 times with respect to the corresponding linear techniques) in a wide range of applications, including elasticity, material characterization, ultrasonics, geophysics to maintenance and restoration of artifacts (paintings, stone buildings, etc.). The book has three parts: Part I - defines and describes the concept of NCNL and its universality and reviews several fields to which it may apply; Part II - describes the phenomenology, theory, modeling and virtual experiments (simulations); Part III - discusses some of the most relevant experimental techniques and applications. The LDRD and DOE Office of Basic Energy Sciences (BES), Geosciences supported the LANL authors.

**Recent Publication highlighted in Discovery Channel News Story, “Why Supercontinents Self-Destruct”**

Continental flood basalts, among the largest volcanic events on Earth, may sometimes form solely in response to the blanketing effect of supercontinents. These findings are reported by Benjamin Phillips (EES–6/11) and colleagues in the May, 2007 issue of ***Geology*** (N. Coltice, B.R. Phillips, H. Bertrand, Y. Ricard, P. Rey, 2007, “Global Warming of the Mantle at the Origin of Flood Basalts over Supercontinents,” ***Geology***, v. 35, p. 391–394) and highlighted in a recent Discovery Channel News story (“Why Super-continents Self-Destruct”, http://dsc.discovery.com/news/2007/05/01/supercontinent_pla. html?category=earth). Phillips is a Director’s Postdoctoral Fellow.

Continents episodically cluster together into a supercontinent. The breakup of supercontinents is often associated with intense magmatic activity at the origin of continental flood basalts. This temporal coincidence, together with domal uplift of the lithosphere and subsequent hotspot tracks rooted in the breakup sites, has led to the hypothesis that a deep mantle plume head could soften the lithosphere, initiate rifting, and trigger continental flood basalt emplacement. The largest Phanerozoic continental flood basalt on Earth (~10 million km2) is the Central Atlantic Magmatic Province (CAMP), which was emplaced with a peak rate 199 million years ago during the initial breakup of the supercontinent of Pangea. CAMP is often cited as a reference example of a plume-derived continental flood basalt, yet this hypothesis is severely debated due to the spatial distribution and chemistry of the lavas and the lack of an identified hotspot track.

Coltice *et al.* propose an alternate non-plume model for the generation of the CAMP on the basis of numerical simulations of mantle convection involving continents. They show that continental aggregation favors longer length scales of flow and naturally generates a broad subcontinental

warming of 100° C without the involvement of hot, active plumes (see Figures). Such a large-scale thermal anomaly would be sufficient to trigger partial melting beneath the supercontinent, especially if the lithospheric mantle were hydrated. While the plume model fits the observations for typical traps like the Deccan in India (high rate of magma supply producing a thick lava pile, hotspot track), the global warming model accounts for the characteristics of the CAMP (wider surface area but thinner lava pile, no hotspot track). The researchers propose two end members: (1) plume-derived and (2) global warming-derived continental flood basalts.

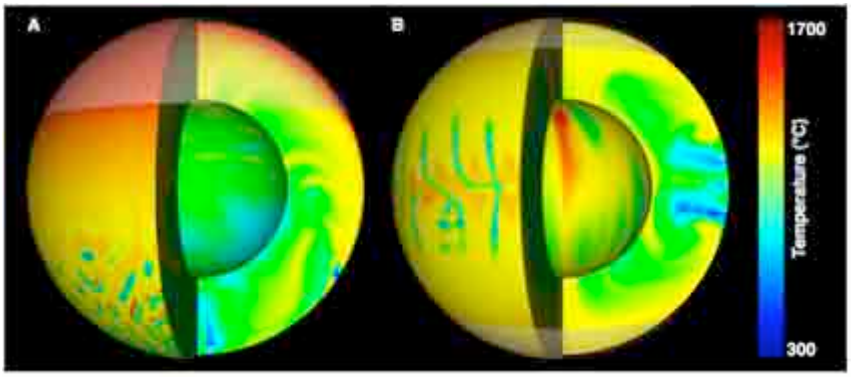


*Figure: Temperature field snapshots for models with (A) a supercontinent and (B) two antipodal continents. The mean temperature at the base of the continental thermal boundary layer in (A) is 1614 ºC (red), while in (B), it is only 1475 ºC (yellow). Translucent caps denote continent locations. Linear features on planetary surfaces delineate regions of cold, subducting*

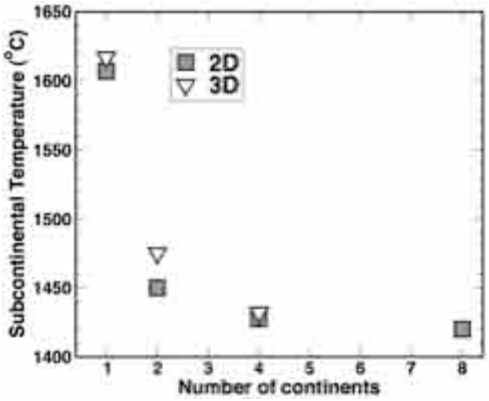


*Figure: Subcontinental temperature (averaged over 1 billion years (Gyr) for three-dimensional calculations and 5 Gyr in two-dimensional calculations) as a function of the number of continents at constant continental area (30%). Significant warming occurs when there is a single continent.*

**Paper published on First Reported Detection of Meteors Via Infrasound and Seismic Signals**

Historically, most of the infrasonic recordings from bolides (exploding meteors) have been from quite large meteors at low altitudes. (Infrasound has a frequency too low to be detected by the human ear.) Doug ReVelle (EES-11) and collaborators P.G. Brown and W.N. Edwards (University of Western Ontario); and P. Spurney (Ondrefov Observatory, Czech Republic) have published a paper in which they examined new infrasonic data recorded in an extremely low background noise site in Freyung, Germany. The measurements were made in conjunction with numerous ground-based photographic camera stations operated as a part of the European Fireball Network (EFN). In 2 years of data analysis for this quiet site, the researchers found four events that absolutely correlate with meteor sources photographed by the EFN (consistent in their timing, directional arrival angles—azimuth and elevation, source energy, optical luminosity, etc.).

Four very high-velocity and high-altitude meteors (a Leonid, two Perseids, and a high-speed sporadic fireball) were detected at the ground, both optically using precision all-sky cameras, and acoustically via infrasound and seismic signals. Infrasound arriving from altitudes of over 100 km is uncommon, but has been observed for re-entering spacecraft. This was the first reported unambiguous detection of such high-altitude infrasound from meteors. The fragile meteoroids generated acoustic waves at source heights ranging from 80 to 110 km. Average source energies for three of the four events from acoustic data alone are in the range of 2 x 10 8-9 J. The character of the shock production for the four events is consistent with a ballistic (cylindrical) shock produced along the entire path of the body entry, as opposed to the quasi-spherical acoustic radiation expected for fragment-type shock production. This is not surprising, given the relatively small mass (<1 kg) of the fireballs studied. The researchers combined the data to model the four entries using the LANL bolide luminosity and detection model (BLDM) modeling code, and they also analyzed the infrasound arrivals using Matseis/InfraTool (data processing software). In a planned second paper they will also produce ray tracings of the signals from these line sources along with detailed acoustical dissipation analyses, since these signals emanated from heights ranging from 90-125 km above the ground. In the third planned paper, they will analyze seismic signals from these same four meteors. The first paper, "Acoustic Analysis of Shock Production by very High-altitude Meteors—I: Infrasonic Observations, Dynamics and Luminosity," was published in the ***Journal of Atmospheric and Solar-Terrestrial Physics*** (**69**, 600-620, 2007). DOE NA-22 supported LANL's infrasound research.

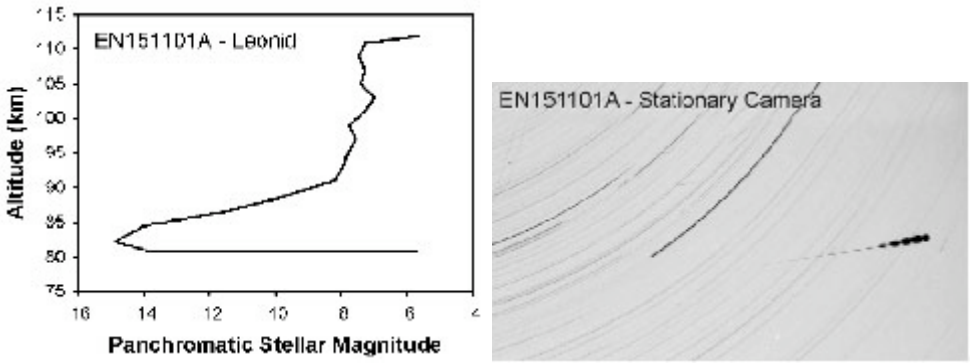


*Figure Left: European Fireball Network image of the Leonid high-altitude meteor from which infrasound has also been measured. Right: Panchromatic lightcurve of the same fireball. The lightcurve was derived from densitometry measurements of the original film records.*

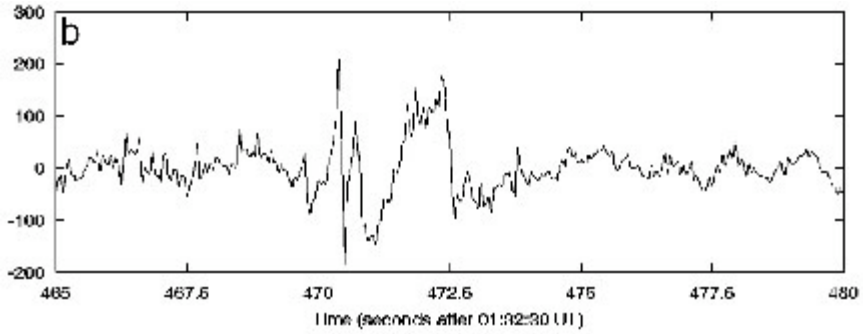


*Figure: Infrasonic pressure wave as recorded by microbarometers for the same Leonid high-altitude meteor.*

**Research on the link between ocean warming and gas hydrates published in a special issue of *Journal of Petroleum Science and Engineering***

Chung-Chieng A. Lai (EES-2) published an invited paper titled, "Effects of gas hydrates on the chemical and physical properties of seawater," **56**, 47-53 (2007), in the ***Journal of Petroleum Science and Engineering***. His paper describes the important role of gas hydrates in the ocean warming and climate dynamics. The global atmospheric warming presents a maximum increase of air temperature at (near) the earth surface where the majority of insolation (*in*flux of *sol*ar radi*ation*) is converted into heat. Ocean observations during the last 50 years show that there is an oceanic warming also. However, the place of maximum warming is not at the ocean surface. Instead, it happens at 400 m depth in the Pacific and at 400 m and 750 m depths in the Atlantic. The warming at the ocean surface is secondary. This implies that the mechanism for ocean warming is different from that for atmospheric warming. Traditionally, climate researchers have not believed that the ocean's internal heat generator, if any, can create a noticeable warming of seawater. This paper not only explains the mechanism, but also presents the evidence found in World Ocean Circulation Experiments (WOCE) data.

A variety of gases can form hydrates within the temperature and pressure ranges of seawater. Huge deposits of oceanic methane hydrate (MH) exist on the seafloor on continental margins. After MH breaks off from sediments, it slowly ascends because its density is slightly less than seawater's. Similarly, nitrogen hydrate is expected to exist in seawater. Further, these gases can form the most common binary hydrates, i.e., methane-nitrogen hydrate (MNH). MNH transforms into water and methane ($_{CH4)}$ and nitrogen ($N_2$) in bubbles when it dissociates at a depth of ~750 m in seawater with a normal temperature profile. Similarly, MH dissociates at a depth of ~400 m. The $CH_4$ may be oxidized (via bacteria) into carbon dioxide ($CO_2$) and releases 810,000 J of heat per mole of $CH_4$ before the bubbles rise to sea surface or dissolve into seawater again. The $N_2$ can be fixed into ammonia ($NH_3$) by microbes and then oxidized into nitrate (NO3-). These biochemical processes deplete the oxygen ($O_2$) dissolved in seawater and generate heat that warms the seawater. Analysis of the relationship among seawater temperature, "apparent oxygen utilization" (AOU) and the concentration of $CO_2$, based on WOCE data, reveals most characteristics that are part of a stoichiometry relation (Figure). But, some are not. Analysis of individual station-profiles confirms that the dissociation of gas hydrates occurs according to temperature and pressure (depth) at hydrate phase boundary. Further, the oxygen utilization derived from the concentrations of dissolved $CO_2$ and $NO_3$- matches the AOU very well at a depth greater than the level where hydrates dissociate. The calculated oxygen utilization is slightly less than AOU in the layer of seawater above the level where hydrates dissociate. This is attributed to the escape of $CO_2$ into the atmosphere after it is produced by oxidation reaction. In short, gas hydrates and the microbes play very important roles in altering the chemical and physical properties of seawater and thus affecting the course of climate change. For more information http://dx.doi.org/10.1016/j.petrol.2006.03.030

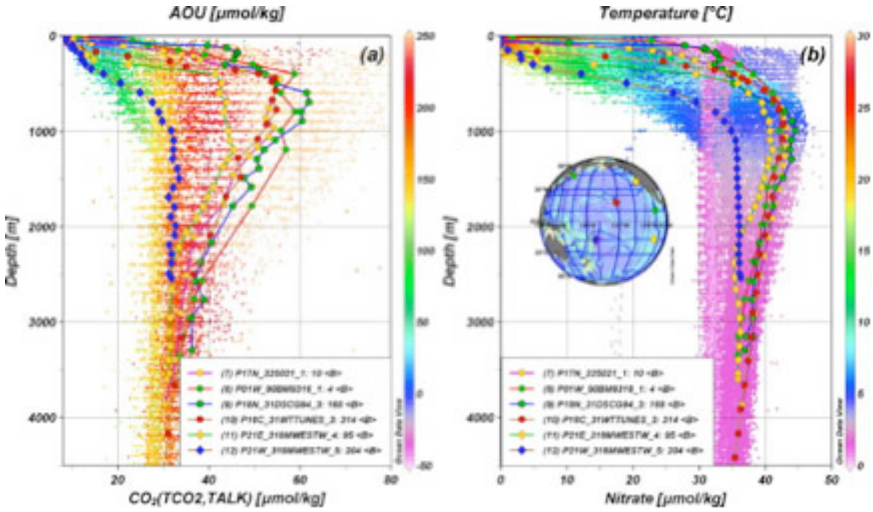


*Figure: Scatter plots superimposed with vertical profiles of (a) [$CO_2$] (with AOU), and (b) [nitrate] (with temperature) for 6 stations in Pacific (shown in the map). [$CO_2$] and [nitrate] represent the concentrations (in µ-mol/kg) of dissolved $CO_2$ and nitrate in seawater, respectively. The vertical color bar on the right side of each panel gives the scale of the magnitude of the variable identified on top of each panel (AOU for panel (a), Temperature for panel (b)). The 6 stations are selected according to a set of requirements to be representative of the whole Pacific Ocean.*

**Successful case study in application of geophysics to groundwater**

Increasingly, concerns about contamination of groundwater resources and the quest for new sources of groundwater drive social and political decisions. To improve the ability to quickly and cheaply characterize groundwater quality and resources, remotely sensed geophysical techniques are being employed. In 2001, EES scientists flew an electromagnetic survey of part of the Pajarito Plateau to characterize local aquifers and contamination pathways. Electromagnetic methods image the electrical resistivity, which is highly sensitive to groundwater, of the outer Earth. The platform was a deHavilland Dash 7 four-engine aircraft carrying a large coil of wires energized by an alternating current (Figure below). The results, when interpreted with existing geochemical and geophysical borehole data, showed "wet" and "dry" areas of the Plateau to depths of 1000 feet or more, and infiltration beneath some canyons. The work provides a baseline for future detailed studies. When the airborne electromagnetic induction analysis is combined with borehole geologic, hydrologic, and geochemical data, it can provide relative depths to saturated zones, delineate regions of high clay content (zones of alteration), and image regions of recharge to the regional aquifer. The survey, an important case study of the method, was published in ***Geophysics*** [W. S. Baldridge (EES-11), G. L. Cole (EES-9), B. A. Robinson (SPO-CNP), and G. R. Jiracek (San Diego State University)], "Application of time-domain airborne electromagnetic induction to hydrogeologic investigations on the Pajarito Plateau, New Mexico, USA," v. 72, pp. B31-B45, 2007). The DOE LANL Environmental Restoration Project and the LANL Groundwater Protection Program supported the work.

*Figure: DeHavilland Dash 7 aircraft, belonging to Fugro Airborne Surveys (Ottawa, Canada), equipped with MEGATEM time-domain electromagnetic induction system for ground-resistivity measurements.*

**Study of tectonically controlled, time-dependent basaltic volcanism published**

Urbanization and construction of long-term facilities in basaltic volcanic fields creates an important class of volcanic risk assessment problems. Understanding the evolution of basaltic volcanic fields is critical to the understanding of basaltic magmatism and to volcanic risk assessment. Estimation of event probabilities in basaltic fields that are dominated by monogenetic volcanoes requires forecasts of both the recurrence rates (or timing) and locations of future events.

Greg Valentine (EES-6) and Frank Perry (EES-9) have published research regarding volcanism in the Southwestern Nevada Volcanic Field (SNVF), an example of an extremely low volume-flux end member of basaltic fields. The SNVF is the geographical area where the proposed Yucca Mountain radioactive waste repository is located (Figure map). The researchers describe physical volcanological data that provide insight into the length scales of sources tapped for each volcano, the lengths of feeder dikes that transport magmas to the surface, and the relationship between lava effusion rates, dike lengths, and volumes at individual volcanoes. Relationships between age and cumulative eruptive volume indicate that the repose interval between eruptive episodes is determined by the volumes of prior episodes. Since approximately 3Ma, the field appears to be time-predictable.

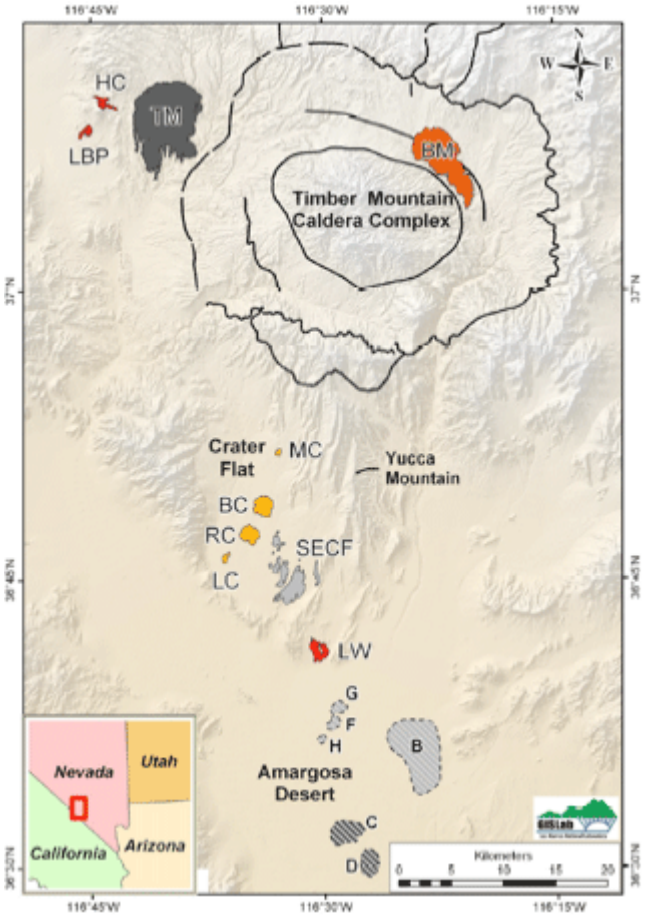


*Figure: Shaded relief map of the southwestern part of the Southwest Nevada Volcanic Shield showing Plio-Pleistocene volcanoes (buried volcanoes in the southern part of the map are indicated with white diagonal line patterns). Color patterns indicate basalts <3 Ma and gray scale patterns indicate>3 Ma. 4.6Ma episode — Thirsty Mountain (TM) and Anomalies C and D. 3.8 Ma episode — SE Crater Flat (SECF) and Anomalies B, F, G, and H. 2.9 Ma episode —Buckboard Mesa (BM). 1.1 Ma episode — Makani volcano (MC), Black Cone (BC), Red Cone (RC) and NE and SW Little Cones (LC). 350ka episode — Little Black Peak (LBP) and Hidden Cone (HC). 77 ka episode — Lathrop Wells volcano (LW). Crater Flat and Amargosa Desert are major basins that host many of the Plio-Pleistocene basalts. Black lines are Miocene caldera boundaries.*

The data support a model wherein magmatism in the SNVF is a passive response to relatively slow regional tectonic strain. Partial melt resides in pockets of lithospeheric mantle that are relatively enriched in hydrous minerals. Slow deformation focuses melt, occasionally resulting in sufficiently high melt pressure to drive dikes upward and feed eruptive episodes, which relieve local stresses. Larger events are followed by longer repose intervals required to recover crustal stresses. The scientists suggest that time-controlled predictability may be a fundamental property of tectonically controlled basaltic fields, where melt accumulation and ascent are controlled by tectonic strain rate. However, time-predictability in a tectonically controlled field does not, by itself, constrain the location or size of potential future episodes. The authors have previously shown that volcano location in the low-flux SNVF depends primarily upon the location and areal extent of the mantle source that is tapped (magma footprint) and secondarily upon shallow structure and surface typography. Because most of the basaltic episodes (except the ~2.9 Ma Buckboard Mesa event) have returned to the vicinity of the existing cluster, the researchers suggest that the magmatic footprints of future events will probably also occur near or within these clusters. Furthermore, general similarities in volcano size and eruptive styles during the past ~1.1

Myr suggests that the future events during the next 100s of kyr will have similar characteristics. All of these factors form potentially important aspects of probabilistic risk assessment in the SNVF. The DOE Yucca Mountain Project supports the work. Reference: Valentine, G. A., Perry, F. V. "Tectonically Controlled, Time-predictable Basaltic Volcanism from a Lithospheric Mantle Source (central Basin and Range Province, USA), ***Earth Planet. Sci. Lett***. (2007) doi, 10.1016/j.epsl2007.06.029

**Advances in carbon capture and storage technologies published**

The potential reactivity of Portland cement in wellbores is one of the key issues in assessing the long-term viability of storage of $CO_2$ in geologic formations. $CO_2$ is known to react with Portland cement, and the possibility of deleterious reactions leading to leakage of $CO_2$ is a serious concern.

LANL has attacked this problem using field, experimental, and modeling methods. Researchers J. W. Carey, S. Chipera, R. Pawar, P. Lichtner (all in EES-6); M. Wigand (C-CSE); G. WoldeGabriel (EES-9); G. D. Guthrie (SPO-FE); R. S. Wehner; and M. Raines obtained the first-ever samples of wellbore systems with exposure to $CO_2$. This provided key insights into wellbore performance that demonstrated for the first-time that the Portland cement may be more robust than was originally thought. Reference: Carey, J. W., Wigand, M., Chipera, S., WoldeGabriel, G., Pawar, R., Lichtner, P., Wehner, S., Raines, M., and G. D. Guthrie. (2007) "Analysis and Performance of Oil Well Cement with 30 Years of $CO_2$ Exposure from the SACROC Unit, West Texas, USA". ***International Journal of Greenhouse Gas Control*** 1: 75-85.

*Figure: The polished surface of a sample of wellbore cement recovered from the SACROC $CO_2$-enhanced oil recovery field (about 5 cm in height). The orange-altered cement reflects reactions with $CO_2$ and is separated from unaltered gray cement by a translucent deposit of silica. This is the first sample of cement ever recovered for studies of long-term $CO_2$ interactions and the security of geological storage of $CO_2$.*

Carey and Lichtner conducted innovative experiments on simulated wellbore systems involving flow of high pressure $CO_2$-brine mixtures through composite cement-caprock and cement-casing systems. The scientists used the results of these experiments to guide their modeling efforts. They found that they needed to significantly enhance existing reactive transport codes to handle solid solution. The researchers published the first reactive transport code capable of handling arbitrarily complex solutions, allowing them to handle both major compositional variation as well as trace contaminants in cement system. Reference: Lichtner, P. C. and Carey, J. W. (2006) "Incorporating Solid Solutions in Geochemical Reactive Transport Equations using a Kinetic Discrete-composition Approach". ***Geochimica Cosmochimica Acta*** 70: 1356-1378.

Using this theoretical foundation, the Carey and Lichtner developed a numerical model for wellbore cements exposed to $CO_2$. They employed this model to predict long-term performance of Portland cement and have thus made significant contributions to the development of Carbon Capture and Storage technologies. These successes have made LANL a recognized leader in

wellbore issues. Reference: Carey, J. W. and Lichtner, P. C. (2007) “Calcium Silicate Hydrate (C-S-H) Solid Solution Model Applied to Cement Degradation using the Continuum Reactive Transport Model FLOTRAN”. In Mobasher, B. and Skalny, J., editors, ***Transport Properties and Concrete Quality: Materials Science of Concrete***, Special Volume, pp. 73-106. American Ceramic Society; John Wiley & Sons, Inc. LANL researchers organized the international Wellbore Integrity Network and hosted the most recent meeting of the Network in March.

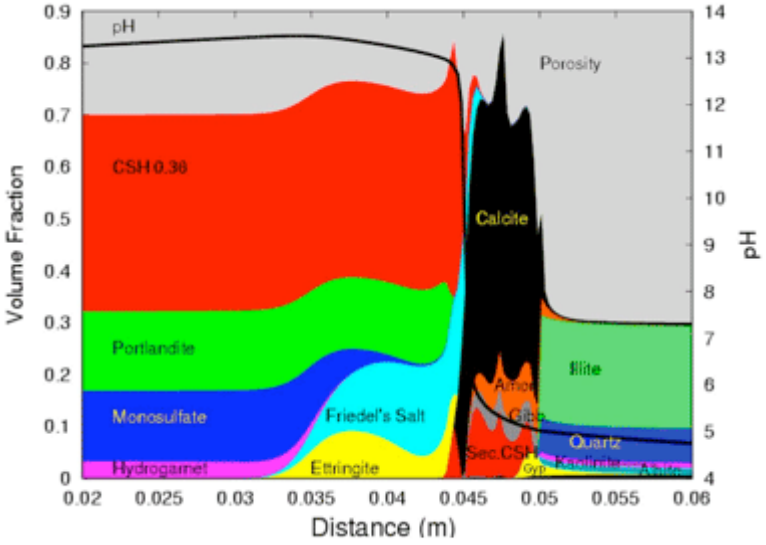


*Figure: Primary Plot: Numerical simulation of $CO_2$-cement reactions occurring within the wellbore environment. The simulations reproduce the key features of the sample of cement recovered from the SACROC site including a 0.5 cm zone of intense carbonation, a region of non-altered cement, and a barrier between the two that impedes further reaction.*

**Detecting Accumulated Damage in Human Bone**

Bone micro-damage is commonly accepted as a relevant parameter for fracture risk assessment in osteoporosis, but there is no available technique for its non-invasive characterization. Currently the x-ray bone density scan is used, but it offers very little information about bone damage.

Paul Johnson (EES-11) and colleagues at the University of Paris Medical School and the Ecole Normal Superier in Paris are developing new methods for diagnosis and following the evolution of osteoporosis. The researchers' objective is to examine the potential of nonlinear ultrasound for damage detection in human bone. Ultrasound is particularly desirable due to its non-invasive and non-ionizing characteristics.

The researchers' experiments explored progressive fatigue damage in human bone samples and methods to measure the damage. The team correlated the progressive fatigue of human bone samples to their nonlinear dynamical response. As damage accumulates during cycling, the measured nonlinear parameter was much more sensitive to damage than were standard measures. Using nonlinear parameter measurement techniques that were developed at LANL, this study represents the first application of the concept of nonlinear dynamic elasticity to human bone. The results are promising, suggesting the value of further work on this topic. Ultimately, the approach may have merit for *in vivo* bone damage characterization, especially for applications related to osteoporosis. The research, "Nonlinear Ultrasound Can Detect Accumulated Damage in Human Bone," by M. Muller, D. Mitton, M. Talmant, P. Johnson, and P. Laugier was published in the March, 2008 issue of the *Journal of Biomechanics.* Marie Muller, the first author, was a student at LANL in 2006. LDRD supported the LANL research.

**Times Marches Backwards - Time Reversal in *Acoustics Today***

An article entitled "Time Reversal", written by Brian E. Anderson, Michele Griffa, Carene Larmat, and Paul A. Johnson of EES-11, was featured as the cover article in the January 2008 issue of *Acoustics Today,* a publication of the Acoustical Society of America. The article describes the basic physics of time reversal (TR) acoustics, its advantages and limitations, and reviews the main application areas of this exciting field of research. The article states, "Reversing time has been a compelling idea for ages. Today we can perform time reversal, leading not to the fountain of youth, but to very interesting physics and applications."


Potential applications include underwater acoustics, biomedical ultrasound imaging and therapy, nondestructive evaluation, and seismology. LANL researchers and collaborators are developing applications to a variety of geophysical problems from the field scale to the global scale. For example, scientists are investigating approaches for land mine detection using time reversal and nondestructive evaluation of solids for crack imaging. At a global scale, time reversal mirror (TRM) has been used to find earthquake source locations by taking the recorded seismograms, time-reversing them, and back propagating them through a numerical velocity model. In the figure below, seismograms were recorded worldwide from the 2004 Parkfield Earthquake in California. The figure shows progressive snapshots of the back propagation of the velocity wavefield. The accuracy of reconstructing an earthquake source using TR relies upon the accuracy of the numerical modeling. With the development of efficient wave-propagation methods that can handle complex geologic models, the TR method is now an alternative to other source location methods. LDRD-DR supports the LANL research.

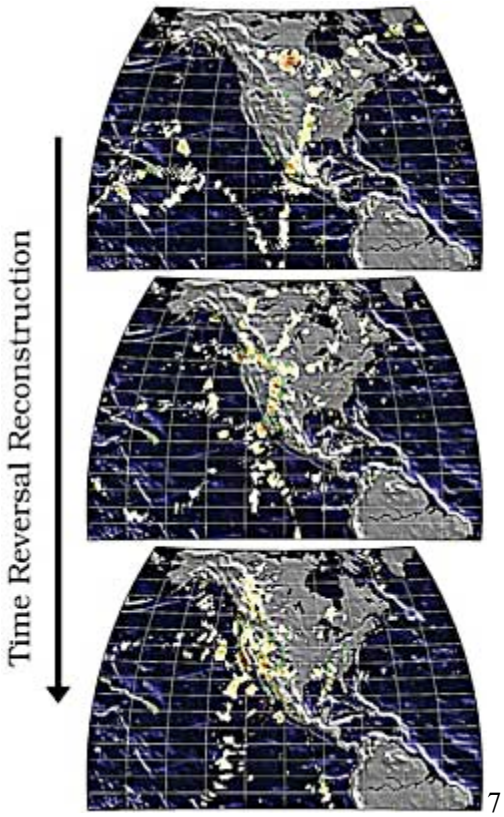


*Figure: Images displaying the Time Reversal reconstruction of the 2004 Parkfield, CA earthquake. From top to botto m the images show the progressive reconstruction of the earthquake as the back propagated wave fronts coalesce at the original source location. This figure was made with the help of GMT software.*

**Upscaling Pore Scale Reactive Transport Modeling to the Continuum Scale**

Multiphase flow and reaction in porous media are among the most complex and challenging problems in water resources research. Although pore-scale interfacial phenomena govern the key processes of fluid mobility, chemical transport, adsorption, and reaction, spatial heterogeneity at the pore scale cannot be resolved at the continuum scale where averaging typically occurs over length scales larger than typical pore sizes. An open question is how important spatial heterogeneity at the pore scale is on the observed behavior at the larger scale. Resolving pore-scale heterogeneity may explain some of the discrepancy between lab-measured and field-derived rate constants, as well as other issues leading to failure of macroscale models. To quantitatively investigate the effects of pore scale heterogeneity on the emergent behavior at the field scale, it is necessary to understand multiphase flow, transport, and reaction processes at the pore scale and subsequently upscale the results to the continuum scale.

Researchers Qinjun Kang (EES-6), Peter Lichtner (EES-6), and Dongxiao Zhang (USC) recently improved the lattice Boltzmann pore-scale model for multicomponent reactive transport in porous media pioneered by them. In the improved model, solute mass is strictly conserved by heterogeneous reactions. The new model was published in *Water Resources Research* (WRR) in November 2007.

In another paper published in WRR in December 2007, Lichtner and Kang presented ground-breaking work on upscaling pore-scale reactive transport equations to the continuum scale using a multiscale continuum formulation. In general a multiscale continuum formulation is required to fit the upscaled pore-scale results. The scientists suggest that a multiscale continuum approach

may help explain the observed discrepancy between laboratory and field-derived reaction rates by explicitly representing distinct transport domains through separate interacting continua. DOE, Biological and Environmental Research and LDRD/DR supported the research.

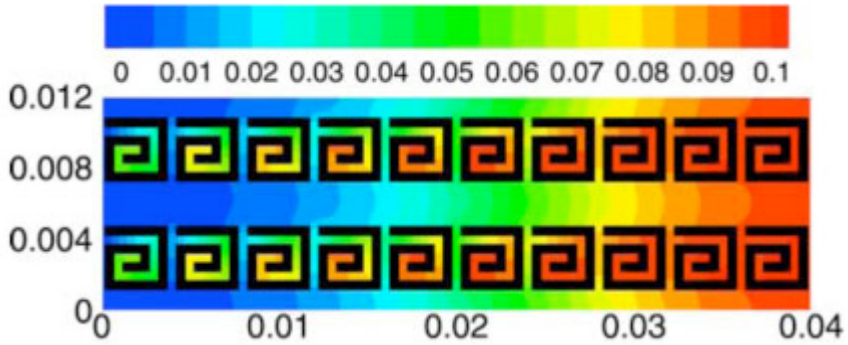


*Figure: Leaching of a tracer initially emplaced at time t = 0 in a two-dimensional structured porous medium (x axis horizontal and y axis vertical) with primary and secondary porosity for a domain size of 0.04 m x 0.012 m. The initial concentration in the primary continuum and matrix fluids is set to 0.1 mol/L.A fluid containing zero tracer is injected at the entrance on the left. The figure corresponds to an elapsed time of 2.6 x $10^4$ s. The black spirals have zero porosity. Concentration units are mol/L.*

**Research on Acoustic-Gravity Waves from Bolide Sources Published**

Douglas ReVelle (EES-2) constructed a model for the generation and propagation of acoustic-gravity waves (AGW) from bolide sources (exceptionally bright meteors). The overall goal is to predict the AGW waveform and the properties of the bolide sources. The model is linked at the source to satellite optical luminosity data to generate a reliable line source and blast wave relaxation radius. Beyond about 10 blast wave radii (near-field region), the model is linked to the well-known weak shock solutions for the amplitude and the wave period of the AGW radiated by the bolide in the continuum flow regime.

Infrasound is the high frequency part of the full AGW spectrum of atmospheric waves. Beyond this limit the far-field wave pulse is linked to three well-known analytic solutions depending on factors related to the source properties (e.g., line source, blast radius, and altitude of the source) and upon how far away from the source the wave system is being observed. The combination of these separate analytic solutions under numerous differing propagation conditions leads to the final result and was compared with AGW observations. The amplitude of the waveform and its overall pressure wave signature are in good agreement. ReVelle applied this modeling technique to bolides, including Tunguska (the Great Siberian meteor of 1908 over Siberia and the Stony-Tunguska River), the Revelstoke meteorite fall of 1965 over British Columbia, Canada; the 2002 Mediterranean bolide; and the 2004 Antarctic bolide. This technique has an immediate application for modeling the infrasound generation from supersonic/hypersonic rocket sources in the atmosphere. The paper, "Acoustic-gravity Waves from Bolide Sources," is published in *Earth Moon Planet.*

**Numerical Modeling of Seismic Phases in a Spherical Earth Model**

Seismic phases $P_n$ and $S_n$ are refracted waves that traverse the Earth's uppermost mantle and are typically the first compressional- and shear-wave arrivals at distances from ~200 to 1500 km. These phases are commonly characterized as being conical headwaves based on considerations of wave interactions with planar constant-velocity layered structures. However, the propagation of $P_n$ and $S_n$ in the actual spherical Earth is much more complex. As epicentral distance increases, $P_n$ and $S_n$ behavior is strongly influenced by the Earth's sphericity, and formal mapping between plane-layered structures and spherical velocity structures is needed.

Researchers Xiaoning (David) Yang (EES-11) and collaborators at the University of California - Santa Cruz and the University of Alaska - Fairbanks have developed new geometric-spreading models for seismic phases $P_n$ and $S_n$, taking into account effects of the Earth's sphericity. The new models provide better representations of $P_n$ and $S_n$ spreading in the real, spherical Earth than the commonly used standard power-law models (Figure below). This conclusion is supported by synthetic simulations and by the successful application of the model on observed $P_n$ data spanning wide distance ranges in Eurasia to yield reasonable attenuation estimates. The new $P_n$ and $S_n$ geometric-spreading models are useful in common situations where only simple velocity models with uppermost-mantle structure represented as constant velocity half-space are available. The use of these models should result in a smaller error in different applications compared with power-law models. Publication: "Geometric Spreading of $P_n$ and $S_n$ in a Spherical Earth Model", *Bulletin of Seismological Society of America,* Vol. 97, 2053-2065 (2007). NNSA funded the work.

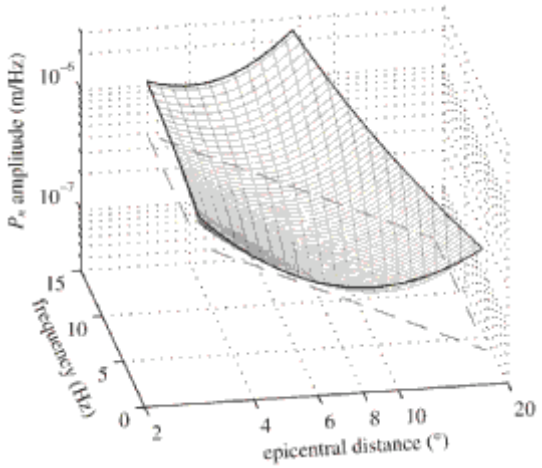


*Figure: Comparison between synthetic amplitudes calculated for a spherical Earth model, the new Pn geometric-spreading model, and a power-law spreading model. The meshed surface is synthetic Pn amplitudes. The white, semitransparent surface bounded by the thick line is the new model. The surface outlined by dashed lines is the power-law model.*

**Dynamic Earthquake Triggering**

Earthquakes happen when Earth's crust slips along cracks called faults. Major faults are found at the junction of independently moving masses of crust and mantle or tectonic plates. Each earthquake releases seismic waves -- vibrations at the cusp or below the range of human hearing -- that travel through the earth. These waves can trigger aftershocks in a zone several to tens of miles away from the radiating main earthquake ("mainshock"). Most aftershocks usually occur within hours to days following the mainshock. The mechanism behind this phenomenon of dynamic earthquake triggering is unknown.

Paul Johnson (EES-11), H. Savage (U. C. Santa Cruz), M. Knuth (U. Wisconsin), J. Gomberg (USGS) and C. Marone (Penn State) conducted laboratory granular friction studies to better understand the physics of dynamic triggering and the influence of dynamic stressing on earthquake recurrence. The researchers used a novel device to examine stick-slip in granular media (glass beads) and applied acoustic waves to simulate earthquake triggering. The experiments demonstrated how wave energy is stored in certain types of granular materials, similar to that found along certain fault lines across the Earth. This stored energy can suddenly be released as an earthquake when hit by relatively small seismic waves far beyond the traditional "aftershock zone" of a main quake. Vibrations also cause large slip events to be disrupted in time relative to those without wave perturbation, suggesting that dynamic stressing of tectonic faults

may play a role in determining the complexity of earthquake recurrence. LDRD and the DOE Office of Basic Energy Research supported the LANL work. The research is published in *Nature,* "Effects of Acoustic Waves on Stick-slip in Granular Media and Implications for Earthquakes" doi:10.1038/nature06440 and in the *Nature* editor's summary.

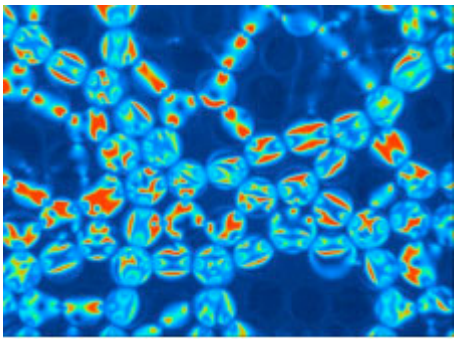

*Figure: Image from Bob Behringer (Duke University) illustrates studies of stress and strain on granular media, similar to what was used in the Penn State University earthquake machine. Stresses on the photoelastic granules in the photo show up as brighter colors, with red showing the regions of highest stress. When forces are applied to granules beneath a plate in the earthquake machine, stresses propagate through the granules, creating "force chains", like the tracks of red visible in the image. Paul Johnson and colleagues showed that force chains break and reform during "earthquakes" induced in the Penn State machine, providing researchers with insight into the periodic behavior of quakes.*

**Low-Level Atmospheric Jets**

Douglas ReVelle (EES-2) and collaborator E. D. Nilsson (Stockholm University) conducted research on low-level atmospheric jets that form in the Earth's atmospheric planetary boundary layer. The researchers' modeling showed that the low-level jets are ubiquitous. The jets can occur all over the globe from quite windy middle and low latitude and quite rough continental locations to the much smoother Arctic and Antarctic oceanic ice-covered regions in the summertime during periods with much lighter wind speeds. This research demonstrates that atmospheric turbulence could be readily maintained over much smoother lower boundaries and at much lower wind speeds (geostrophic winds) than had ever been appreciated before. (Geostrophic winds occur above the friction layer and develop in response to gradients in atmospheric pressure over large regions of the surface of the earth.) This research was published in "Summertime Low-Level Jets over the High-Latitude Arctic Ocean" in the *Journal of Applied Meteorology and Climatology* 47, 1770-1784 (2008).

The success of this analytic model relies on the fact that the predicted turbulence levels over smoother surfaces in the presence of light winds can be approximately three times greater than those over continental locations with rougher lower boundaries and higher reference wind speeds. These turbulence levels are only available in a very shallow layer (< 5 m in vertical thickness) near the earth's surface, whereas somewhat lower turbulence levels are predicted to extend over a much deeper atmosphere layer (hundreds of meters in vertical thickness) in the middle latitudes. These latter conclusions are based upon predictions of the atmospheric surface boundary layer height that the researchers elaborated upon in a recent addendum that was written since the original paper was accepted in *Journal of Applied Meteorology and Climatology*.

**Volcanic Risk Assessment at Yucca Mountain**

*Bulletin of Volcanology* 70: 563-582 (2008).

Gordon Keating, Greg Valentine, Don Krier, and Frank Perry of EES-9 published a paper that quantifies key parameters used to model eruption scenarios for volcanic risk assessment at the

planned Yucca Mountain high-level radioactive waste repository in Nevada. "Shallow Plumbing Systems for Small-volume Basaltic Volcanoes" summarizes field work of eroded analogue volcanoes that were used to characterize the geometry of potential future basaltic conduits through the Yucca Mountain repository. The paper compares field measurements to theoretical considerations of conduit flow in order to draw general conclusions about the size and shape of potential conduits at repository depth (ca. 300 m) and the nature of the transition from dike to conduit at shallow depths.

Quantification of the size and geometry of basaltic conduits has not been done previously at this depth range. This kind of information is critical in the analysis of consequences of a potential basaltic eruption through the waste repository. Given the explicit layout of storage tunnels and the shape and disposition of waste packages, the size and geometry of a magmatic conduit developing at the repository horizon has direct bearing on the number of waste packages damaged and the amount of waste released during a potential volcanic eruption. The quantification of magma conduit geometry developed in this paper provides direct input to the eruptive case submodel of the Yucca Mountain Total System Performance Assessment (TSPA). In a broader sense, the comparison of field observations to conduit geometries developed in the numerical model supports the concept of lithostatic-pressure balanced flow conditions put forth by Wilson and Head (1981). DOE's Yucca Mountain Project funded the research.

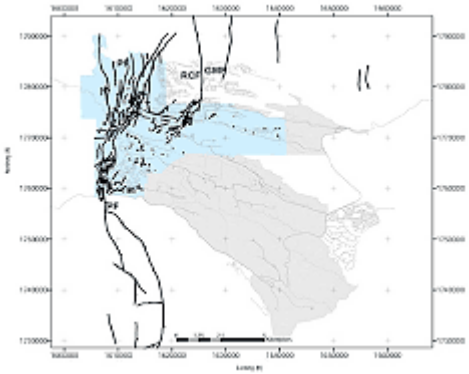

*Figure: Comparison of sketches of three eroded conduit systems for ancient, small-volume basaltic volcanoes. The feeder dike and conduit at East Basalt Ridge is exposed to a depth of 270 m, providing an unusual view of the transition from a smooth-walled feeder dike to a funnel-shaped conduit beneath the eruptive vent (now filled with lava and fragmental material). The transition occurs at a depth of about 90 m as the single feeder dike branches and envelopes fragmented host rock. The sketches of the Paiute Ridge neck and the fissure deposits at Pliocene Crater Flat have been placed in relative vertical position with respect to the East Basalt Ridge sketch.*

**Multiscale Analysis Applicable to Field Scale Simulations**

A major problem in modeling natural porous media is obtaining an accurate description of their flow and transport behavior in spite of the intrinsic heterogeneity of geological formations. The modeling equations have coefficients that vary on scales that are small compared with the overall size of the domain of interest. Any accurate numerical solution of these models requires a very finely divided computational mesh, something that often is not feasible. Obtaining the macroscopic behavior of a given system can become computationally expensive even with modern supercomputers. Therefore, to analyze the system from a macrostructure point of view, it is desirable to simplify it in such a way that the phenomena of interest remain adequately described. The simplified equations are called homogenized equations, and the procedure of replacing the original system is called homogenization.

Researchers Roseangela Svlercoski and Brayan Travis of EES-2 and T-7's James Hyman recently published a paper entitled "Analytical effective coefficient and a first-order approximation for linear flow through block permeability inclusions" in *Computers & Mathematics with Applications,* 55 (9), 2118-2133, (2008). These new results are applicable to idealized geometric form of inclusions in a main matrix. However, the extension to the general case is possible and it is ongoing work. The new results will allow multiscale numerical simulations for field scale applications which is also the new feature of the method.

The LANL researchers have developed an approach that differs from the previous ones, by simplifying the numerics involved in such approximations. The approach has the enormous advantage of portability because it can be used with any existing elliptic solver. Below, the figure shows a comparison of the analytic solution with square inclusion and the relevant numerical approximation. The two graphs agree well with each other but differ on the smoothness.

The ultimate goal is to apply the method to multiphase systems in cases where diffusion is the driving process.

A Chevron-LANL CRADA provided support for the work.

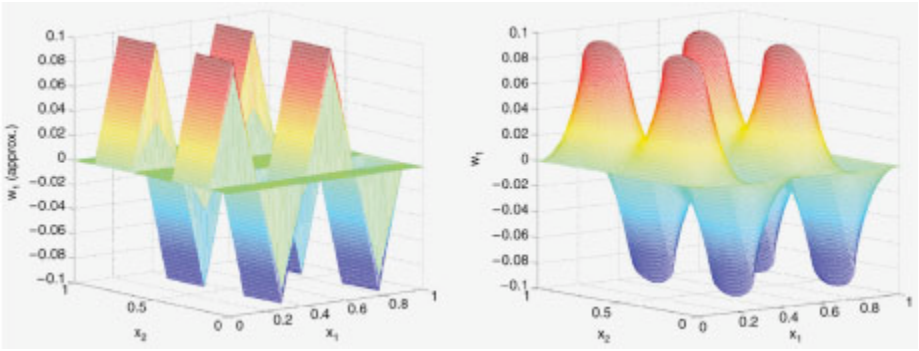

*Figure: Left - Analytical solution with square inclusion. Right - Numerical approximation.*

**Analysis of a Crater-Forming Meteorite Impact in Peru**

Douglas ReVelle (EES-2) and collaborators analyzed the fireball that produced a crater-forming meteorite fall near Carancas, Peru, on 15 September 2007. The researchers used eyewitness, seismic, and infrasound records to investigate the fireball and crater. Several eyewitnesses described the fireball as being nearly as bright as the sun and heard a loud explosion. Although the fall of the meteorite was not recorded optically, global instrumentation provided by the International Monitoring System of the Comprehensive Test Ban Treaty Organization recorded infrasound waves produced by the fireball passage. The meteorite impact, which produced a crater of 13.5 m diameter, released on the order of 1010 J of energy, equivalent to 2-3 tons of TNT high explosives. The scientists calculate the initial mass of the meteoroid to be in the range of 3-9 tons. Their modeling suggests a final end mass for impact on the order a few metric tons and an impact velocity in the 1.5-4 km/s range.

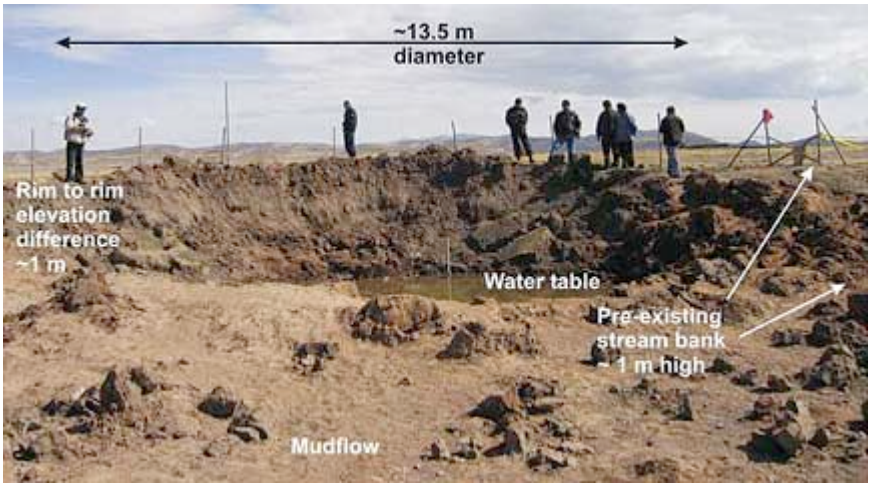


*Figure: The crater 7 days after formation.*

The most unusual aspect of this crater-forming impact is the nature of the impactor. In general, chondritic (stony) meteorites break up during atmospheric flight and do not reach the surface as large objects with a significant fraction of their pre-atmospheric speed. The scientists conclude that a strong, coherent stony object with few shock cracks could withstand the pressures most of their models predict for the meteorite (based on lab measurements of meteorite strengths) and experience mild or no fragmentation as opposed to the catastrophic fragmentation typical for chondrites.

The researchers deduce that the formation of such a substantial crater from a chondritic mass was the result of the unusually high strength (and corresponding low degree of fragmentation in the atmosphere) of the meteoritic body. Additionally, the high altitude of the impact site resulted in an almost one order of magnitude higher impact speed than would have been the case for the same body impacting close to sea level. Modeling suggests that much of the mass of the original impactor spalled out of the crater and/or the mass remaining in the crater is in disaggregated small fragments.

Reference: Brown, P., D. O. ReVelle, E. A. Silber, W. N. Edwards, S. Arrowsmith, L. E. Jackson Jr., G. Tancredi, and D. Eaton "Analysis of a Crater-Forming Meteorite Impact in Peru", Journal of Geophysical Research 113, E09007, (2008).

**Role of Iron in Aging of Polysiloxane Foams**

Chemical degradation of room temperature vulcanized polysiloxane filled foams is an important issue because it can strongly affect mechanical properties and long-term service of these materials. The foams are subject to degradation as a result of aging and environmental conditions. Although these foams generally show low reactivity with oxygen, sunlight, and most chemicals, hydrolysis of the foams in trace amounts of water is a potential concern. While these foams are not hygroscopic, fillers used to reinforce them can absorb water.

Michael Blair (EES-2), Ross Muenchausen (MST-8), Dean Taylor (MPA-10), Andrea Labouriau (MST-7), Wayne Cooke (MST-8, retired), and Tom Stephens (WT-6) conducted electron paramagnetic resonance and Mössbauer spectroscopy to investigate potential aging mechanisms in these filled polysiloxane foams, diatomaceous earth filler, and their other constituents.

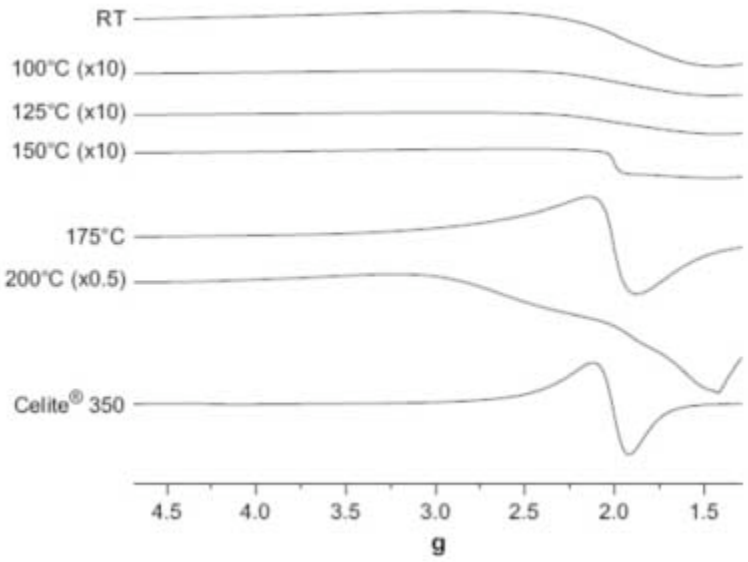


*Figure: EPR spectra, measured at room temperature, of lepidocrocite that has been step-annealed to the specified temperature. The EPR spectrum of Celite® 350 (diatomaceous earth) has also been shown for comparison, and it is clear that annealed lepidocrocite is present in diatomaceous earth.*

These materials are used as stress cushions, and the presence and role of water is particularly important. The study found the presence of intermediate forms of iron oxides in diatomaceous earth fillers and polysiloxane foams indicating that the diatomaceous earth is a marker for the water content rather than directly participating in water cycling in the foams.

The Non-Nuclear Enhanced Surveillance program supported the work. Reference: "EPR and Mössbauer Characterization of RTV Polysiloxane Foams and their Constituents" in Polymer Stability and Degradation 93, 1585-1589 (2008).

**Flow Cytometry Examination of Immune Function in Poultry**

Jeanne Fair (EES-2), Kirsten Taylor-McCabe, Yulin Shou, and Babs Marrone (all of B-7) applied the LANL flow cytometry resources to the immunophenotyping of chickens. Immunophenotyping is a process used to identify cells based on the types of antigens or markers on the surface of the cell. Investigations on the immune response in birds relative to disease resistance and infection is important to the understanding of diseases in the environment and our agricultural resources.

*The work demonstrates that flow cytometry can be used to identify the cell surface molecules (CD or "cluster of differentiation" molecules) that are expressed on white blood cells or lymphocytes. These molecules indicate the different stages of activation of the lymphocytes aiding in a more complete understanding of the overall immune function. The scientists examined the reliability of using these methods to compare chickens raised in different environments and conditions and the reproducibility of the method between commercially available antibodies and labeling reagents.*

This paper is the first in a series of reports describing lymphocyte subpopulations in birds that included a collaboration of a West Nile virus infection study at Colorado State University last fall. This project was assisted by the expertise of Charles Hathcock and David Keller (both in ENV-EAQ). The research, "Immunophenotyping of Chicken Peripheral Blood Lymphocyte

Subpopulations: Individual Variability and Repeatability", is in *Veterinary Immunology and Immunopathology*, 2008, vol. 125, n°3-4, pp. 268-273 [doi:10.1016/j.vetimm.2008.05.012. LDRD supported the research.

**Research on Discharge Physics on Other Planets Published in *Space Science Review***

Robert Roussel-Dupre, Jonah Colman, and Eugene Symbalisty of EES-2 and collaborators D. Sentman (University of Alaska Fairbanks) and V.P. Paska (Pennsylvania State University) published an overview of discharge physics including both conventional and runaway breakdown in atmospheres. The paper discusses transient luminous events and terrestrial gamma-ray flashes in the context of discharge processes on other planets.

The acceleration, scattering, and energy loss or gain experienced by an electron as it moves through a gas subject to an applied electric field depends entirely on the gas composition, the details of the electron interactions with the constituent particles, and the boundary conditions. For weak fields the electrons drift and diffuse through the gas while undergoing elastic and inelastic collisions that together with the field define their momentum and energy distribution. The inelastic interactions that can occur include rotational, vibrational, and electronic excitations of the gas particles as well as losses from attachment and recombination. For stronger fields it is possible for ionizing collisions to take place. A gas discharge is initiated when the applied electric field exceeds the threshold value necessary for a sufficient population of electrons to overcome collisional drag and accelerate to energies beyond the gas ionization potential. In addition the ionization rate must exceed the net dissociative attachment rate (if extant) in order to have a net growth in the electron population. The energy or electric field at which the two balance each other defines the threshold for a discharge to initiate. Three-body attachment may also play an essential role in defining the overall development of the discharge as in air.

Two electrical breakdown mechanisms are known to operate in dielectrics. The conventional breakdown process is recognized as the sparks, arcs, and glow discharges of routine occurrence. The second is a relatively new mechanism called runaway breakdown, involves an avalanche of relativistic electrons that are collimated by the applied field to form an electron beam. Runaway breakdown may play an important role in lightning discharges on Earth.

The authors examine the kinetic theory of electron transport in gases relevant to planetary atmospheres (nitrogen, oxygen, hydrogen, carbon dioxide, methane, and helium) and present results of detailed Boltzmann kinetic calculations for a range of applied electric fields. These calculations are compared with experimental discharge swarm data.

Of the many forms that a discharge can take in the terrestrial environment, lightning is by far the most spectacular and the most dangerous. The amount of energy expended in a single event is generally more than gigajoules with power levels reaching tens to hundreds of gigawatts. The currents that flow in a cloud-to-ground (CG) discharge range in magnitude from hundreds of amps to hundreds of kiloamps and transfer Coulombs to tens of Coulombs of charge. The bulk of this electrical energy flows through small cross-sectional areas with radii ranging from centimeters to tens of centimeters and over long distances extending to many kilometers. The kinetic energy density in lightning is sufficient in many cases to heat the air to tens of thousands of degrees Kelvin and to generate acoustic shock waves that can be heard out to tens of kilometers. Terrestrial lightning is easily observed from the ground and from space in the optical, the radio frequency, and most recently in the X-ray and gamma ray parts of the electromagnetic spectrum. Some of the physical manifestations of the lightning discharge are shown in Figure 1.

The scientists conclude that the precise manner in which an electrical discharge would evolve on a given planet depends on the magnitude and atmospheric profile of the electric fields. The charging mechanisms and the gas density profile are crucial to establishing the conditions that are conducive to gas breakdown. The researchers conclude that under similar conditions runaway

breakdown is more likely to occur on the gas giants such as Jupiter than conventional breakdown when compared to Earth or the other planets. Radiofrequency and gamma-ray emissions from the runaway beam would be highly collimated on the gas giants.

Reference: R. Roussel-Dupré, J. J. Colman, E. Symbalisty, D. Sentman, V.P. Pasko, "Physical Processes Related to Discharges in Planetary Atmospheres", *Space Science Review,* June 2008; DOI 10.1007/s11214-008-9385-5.

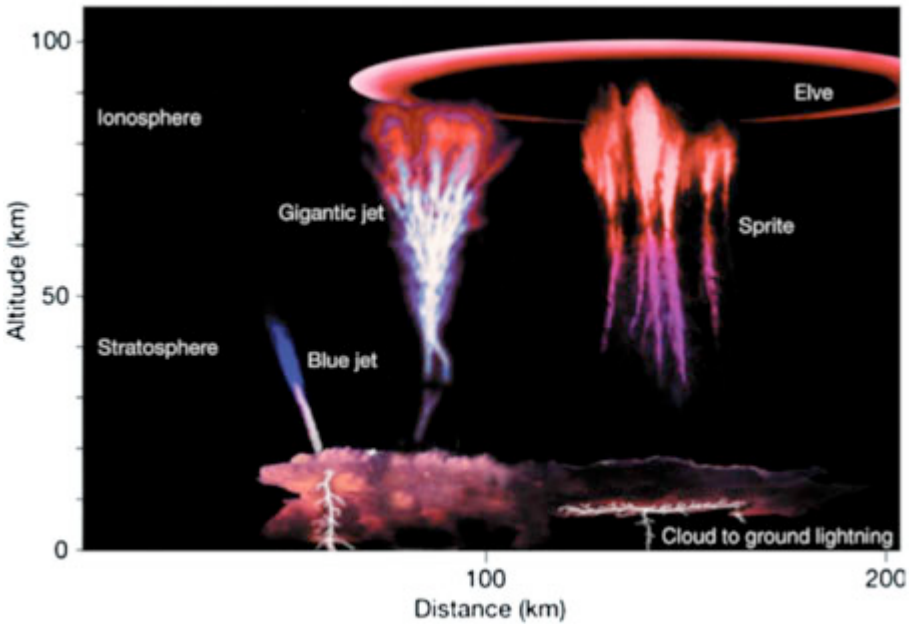


*Figure: Thirteen lightning-related transient luminous events. Several types of these events are known and shown here: relatively slow-moving fountains of blue light known as 'blue jets' which emanate from the top of thunderclouds up to an altitude of 40 km, 'sprites' that develop at the base of the ionosphere and move rapidly downwards at speeds up to 10 000 km s-1, 'elves' which are lightning induced flashes that can spread over 300 km laterally, and upward moving 'gigantic jets' which establish a direct path of electrical contact between thundercloud tops and the lower ionosphere.*

**Determining the Age of the Grand Canyon**

The Grand Canyon's age has remained controversial since the days of John Wesley Powell and has resulted in over a century of scientific controversy. While scientists have reached general consensus that the canyon was probably carved by the Colorado River starting around six million years ago, a recent paper in the journal *Science* claimed to have found rocks in a cave near the western section of the canyon that proved the huge chasm was at least 17 million years old.

David Coblentz and Jolante Van Wijk of EES-17 along with collaborators at the University of New Mexico published a rebuttal paper in the journal *Geology* to help to resolve this debate by

constraining the dynamics of the canyon incision. They developed an incision model that integrates tectonic influences and driving forces such as faulting, mantle to surface fluid interconnections, and mantle-driven dynamic uplift of the western edge of the Colorado Plateau.

The authors argue that a combination of three faults in the area and upwelling hot mantle material pushed the region's rocks upward, causing the canyon to form in segments from east to west over the last six million years (See figure below). The scientist believe that the faulting and uplift have influenced differential incision of the Grand Canyon in the past 6 million years, causing persistently different rates in the western versus eastern Grand Canyon.

These conclusions differ from the traditional view of canyon incision solely through a river passively carving the landscape. This fault evolution and tectonic driving forces are components that must be included in a viable model for the incision history of the Grand Canyon. Metaphorically, it is like cutting a layer cake with a knife. The knife indeed cuts the cake, but there is also a component of the cake rising.

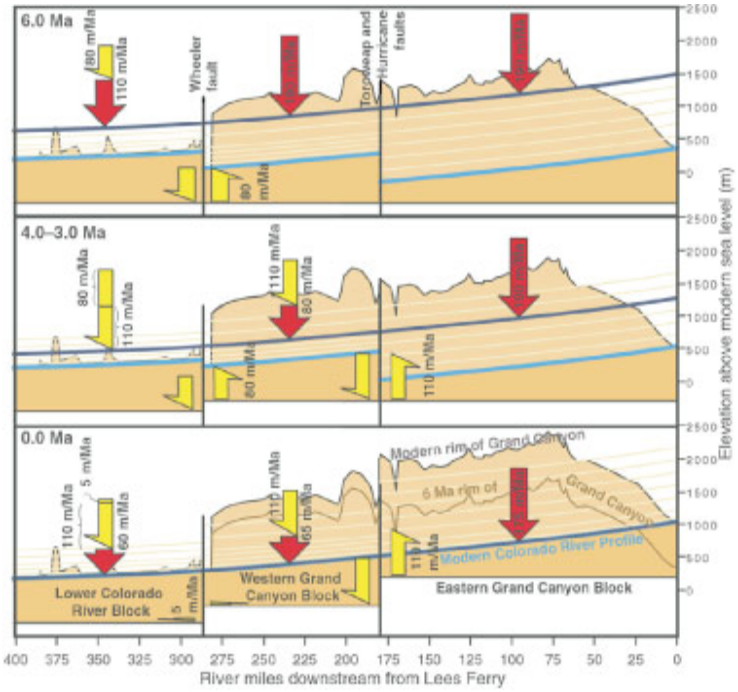


*Figure: Sequential restoration and model constraints for interplay between Grand Canyon incision rates (red arrows) and normal faulting (yellow arrows) in the past 6 million years. Shown here are 3 panels of a 12-panel animation.*

K.E. Karlstrom, R. Crow, L.J. Crossey, D. Coblentz, and J.W. Van Wijk, "Model for Tectonically Driven Incision of the <6 Ma Grand Canyon", *Geology* 36, 835-838 (2008). The LANL research was sponsored mostly through Institute for Geophysics and Planetary Physics (IGPP) and support of yearly Geodynamics of the Western U.S. workshop.

**Simulating the Effects of Aerosol Pollution in Clouds**

The Earth's atmosphere typically contains a mixture of different types of aerosols that are produced by natural or anthropogenic processes. These aerosols play an important role in weather and climate through direct or indirect mechanisms. For example, a direct mechanism involves the ability of aerosol to influence the Earth's energy budget by either reflecting and/or absorbing radiation. However, by serving as cloud condensation nuclei, an indirect process is the impact of aerosol on cloud droplet concentration and also the mean cloud droplet radius and subsequent overall radiation budget. Because of the abundance of stratus clouds over vast stretches of the

Earth's atmosphere, any changes in their mean properties via the indirect effect can have a rather large impact on the Earth's climate. Therefore it is important to understand the impact of pollution via anthropogenic aerosol on stratus clouds.

In a paper published October 10, 2008 in the *Journal of Geophysical Research,* five LANL scientists from three Divisions integrated models, experiments, and observations to successfully simulate the effects of aerosol pollution on clouds. The authors, M. Andrejczuk of EES-2, J. M. Reisner of EES-16, M. Dubey of EES-14, B. Henson of C-PCS, and C. Jeffery of ISR-2, developed a new high-fidelity cloud resolving model with laboratory based parameterization of cloud activation by soot containing aerosols

The model is the first to successfully simulate airborne field observations (DYACOMS-II) of polluted and clean clouds and quantify the "indirect" effect of aerosols on cloud brightness, a key uncertainty in climate assessments. The researchers assessed the impact of changes in aerosol number and composition on stratus clouds. The work resolves a scientific controversy by showing that chemical effects, as well as aerosol particle size, are important in the nucleation of cloud droplets. This new capability supports LANL's climate observations and modeling programs in the DOE Office of Biological and Environmental Research - Office of Science. The researchers are working with PNNL, the Science Focus Area lead, to incorporate the findings into global climate models.

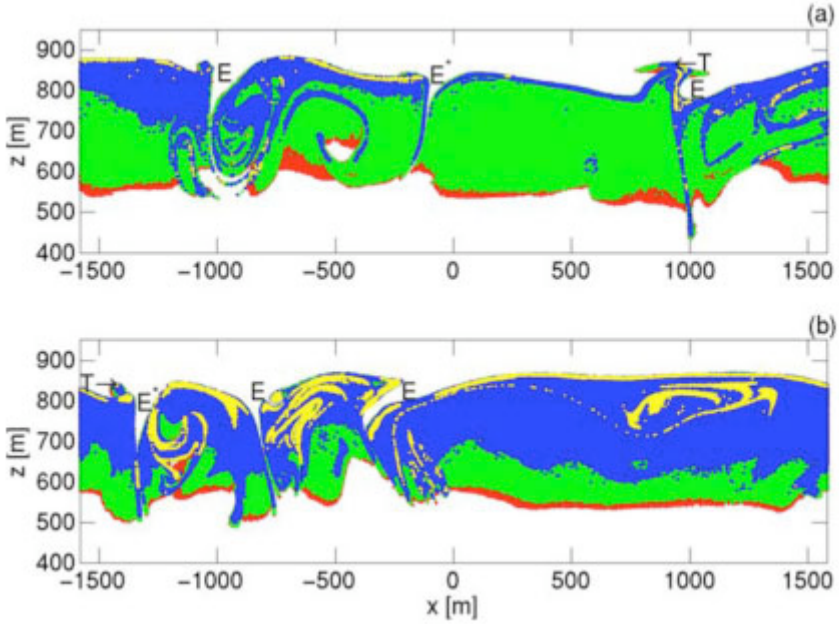


*Figure: Spatial distribution of activated cloud droplets from initial aerosol particles for (a) polluted and (b) clean conditions. The size of the droplets is indicated by colors r < 3 mm (red), 3 mm < r < 9 mm (green), 6 mm > r >9 mm (blue), and r 9 > mm (yellow). It is evident that polluted clouds with hydrophilic aerosols (a) have smaller drops than cleaner clouds and (b) the indirect effect of aerosols on clouds.*

Reference: "The Potential Impacts of Pollution on a Nondrizzling Stratus Deck: Does Aerosol Number Matter More than Type?", Journal of Geophysical Research 113, D19204 (2008). The LANL-LDRD-DR, "Resolving the Aerosol-climate-water Puzzle" (PI-M. Dubey), funded the work.

**New Method for Improving Confidence to Monitor a Comprehensive Test Ban Treaty**

Howard Patton of LANL's EES-17 and a a collaborator developed a new method to study source characteristics of regional phases including explosion-generated S-waves (shear waves). This

method uses differences between spectrograms of two closely located explosions recorded at a common station. Relative source effects of one explosion with respect to another explosion are isolated in the resultant difference spectrogram because path and receiver site effects cancel. This gives a global view of the relative frequency content.

Difference spectrograms for Nevada Test Site explosion pairs Rousanne/Techado and Baseball/Borrego provide information about the spectral content of regional phases related to source effects which can be used to gain insight into source generation processes and improve the confidence to monitor effectively at low yields.

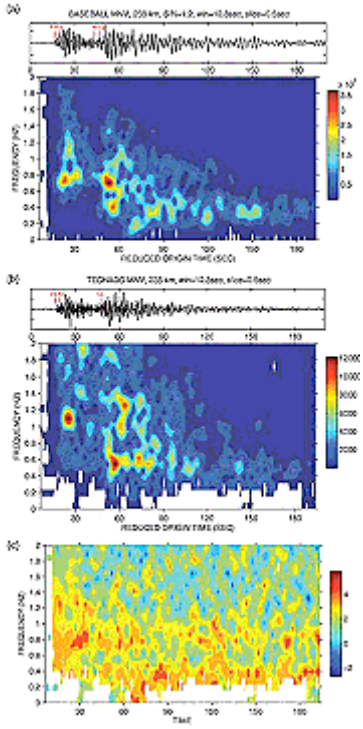

*Figure: Spectrograms of Baseball (a) and Techado (b) explosions and the difference spectrogram [(a) - (b)] in (c). Regional-distance seismograms used in the analysis are plotted above the spectrograms. Cool blue and green colors indicate low amplitudes. Hot colors represent high amplitudes. A signal/noise threshold screens unreliable data, plotted in white. Spectral modulations are revealed by high amplitudes at frequencies below ~0.5 Hz, relatively low amplitudes between 0.5 and 0.7 Hz, high amplitudes between 0.7 and 1 Hz, and generally low amplitudes above 1 Hz. Between 0.5 and 0.7 Hz, the difference spectrogram has a "blotchy" appearance as a function of time down the record, possibly due to scattered arrivals of Rg-derived energy.*

I.N. Gupta and H.J. Patton, "Difference Spectrograms: A New Method for Studying S-Wave Generation from Explosions," Bulletin of Seismological Society of America 98, 2460-2468 (2008).

**Model for Dissolution Driven Convection in Geological Sequestration of Carbon Dioxide ($CO_2$)**

Sequestration of anthropogenic $CO_2$ emissions in saline aquifers is one of the most promising ways of mitigating emissions in the short term. $CO_2$ is a supercritical fluid with a density that is about 30% lower than that of the surrounding brine under the thermodynamic injection conditions. The $CO_2$ rises to the top of the domain under the low-permeability caprock at the top

of the aquifer and begins to migrate laterally, which can lead to leakage into fractures or other wells (below). The $CO_2$ slowly dissolves into the underlying brine. The competition between lateral migration and dissolution plays a key role in determining the leakage risks for an aquifer. Brine with dissolved $CO_2$ is denser than the brine alone, resulting in a gravitational instability. The instability leads to a convective process where fingers of $CO_2$-rich brine penetrate the aquifer and increase the dissolution rate.

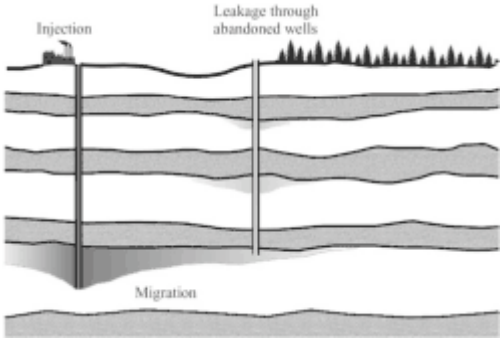


*Figure: Schematic of $CO_2$ injection, migration, and leakage during geologic storage.*

Rajesh Pawar and Philip Stauffer (both in EES-16) and collaborators developed highly accurate theoretical and computational models to understand the onset of the convective process. They used a theoretical approach called "Non-modal Stability Analysis" to study the growth of infinitesimal perturbations over the dissolution process. Previous techniques required the geometric structure of the initial perturbations and used arbitrarily chosen initial conditions as an input. In contrast, Non-modal stability theory is a powerful mathematical tool that can predict the maximum amplification over the entire set of initial perturbations. Scientists obtained, for the first time, the structure of the most-amplified initial condition. They also developed a three-dimensional pseudo-spectral solver for the governing equations to verify the results of the analysis. In the figure below the amplification computed from the spectral solver is compared to that predicted by the stability theory. The growth of perturbations is well predicted by non-modal theory as long as the non-linear terms remain weak. After a certain amount of magnification, the non-linear terms, which were ignored in the non-modal analysis, become dominant. The system transitions into a convective state. Then convection begins to dominate over the slow diffusive process. Non-modal stability calculations are extremely fast compared to full simulations because the computation only involves solving ordinary differential equations and computing singular values of matrices. This approach can be used in conjunction with a "threshold" model to predict the onset of convection. In the plot, convection is expected to begin once the perturbations have amplified by a factor of 1000. The time at which the perturbations saturate (and the process of convection begins) is strongly related to the strength of the initial perturbations.

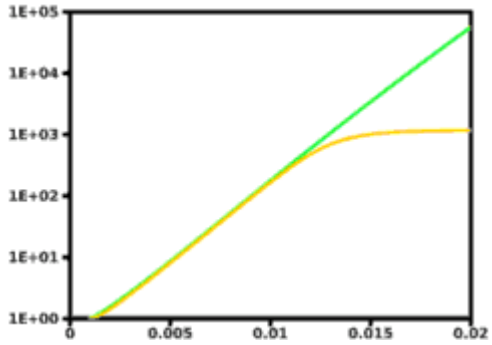

*Figure: Comparison of the amplification of perturbations computed from non-modal theory (green)*
*and spectral simulations (orange) as a function of non-dimensional time.*

This theory also predicts the length scale of the early finger-like structures as shown below. A more rigorous approach would only need the initial strength of perturbations, which could be obtained from suitably designed experiments. Reference: S. Rapaka, S. Chen, R.J. Pawar, P.H. Stauffer and D. Zhang, "Non-modal Growth of Perturbations in Density-driven Convection in Porous Media," Journal of Fluid Mechanics 609, 285-303 (2008). DOE Zero Emissions Research Technology (ZERT) funded the research.

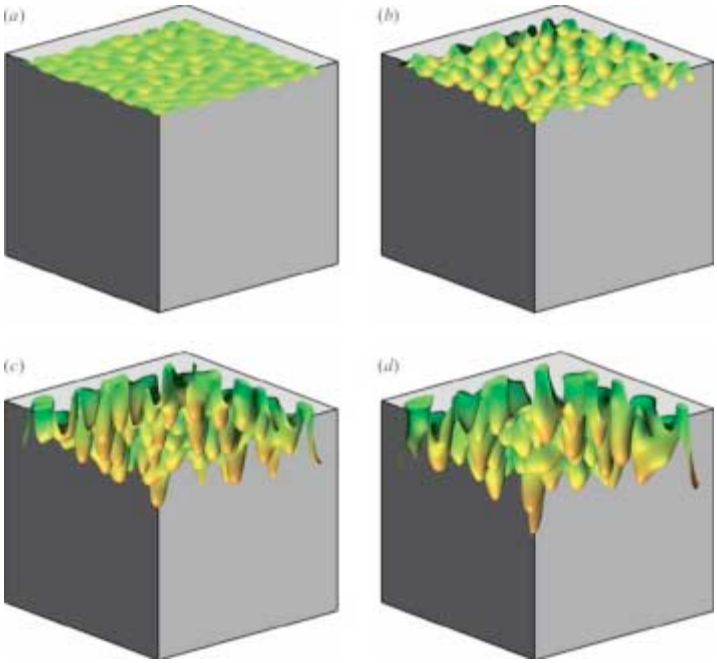


*Figure: Isosurfaces of the concentration of carbon dioxide for a simulation show the growth of "fingering" convection pattern from the spectral simulations as a function of time.*
*The isosurfaces are plotted at (a) $t = 1.59 \times 10^{-3}$, (b) $t = 2 \times 10^{-3}$, (c) $t = 3 \times 10^{-3}$ & (d) $t = 4 \times 10^{-3}$.*

**Novel Technique Developed to Image Earth's Structure**

Monica Maceira (EES-17) and C. J. Ammon (Penn State University) developed a novel technique for simultaneous joint inversion of surface wave velocity and gravity observations to better constrain and image the Earth's structure.

Knowledge of the three-dimensional continental structure is needed to understand crustal generation and its geodynamic evolution. Combining these observations into a single inversion enables a self-consistent three-dimensional (3-D) shear velocity-density model with increased resolution of shallow geologic structures. An iterative, damped least squares inversion including smoothing is used to jointly model both data sets, using shear velocity variations as the primary model parameters. Synthetic data fits to the observations show how the 3-D velocity model obtained from the joint inversion can simultaneously fit both data sets, offering a compromise between fitting both data sets individually.

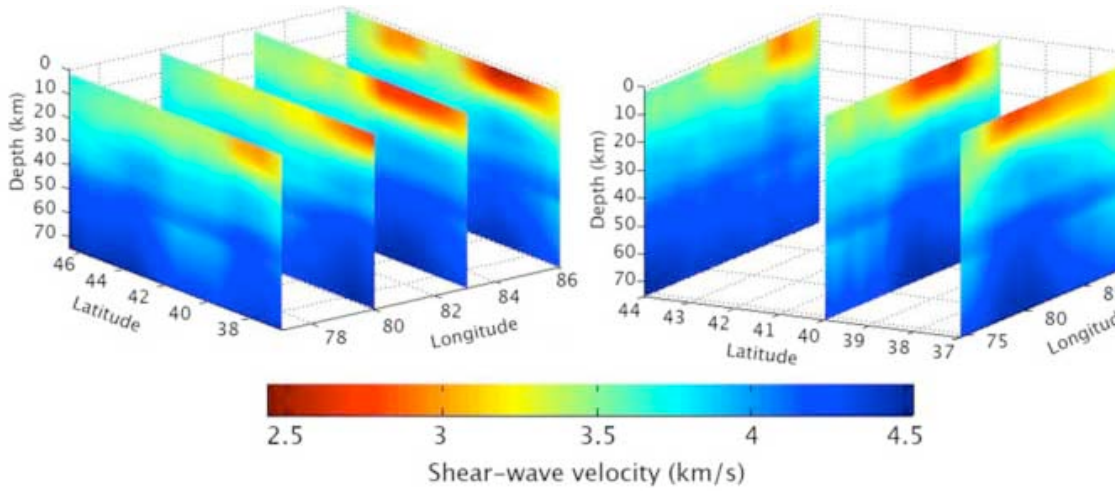


*Figure: Three-dimensional S-wave velocity model at constant longitude (left) and latitude (right) slices. The depth range is indicated on the vertical axis. Warm colors indicate slow velocities meanwhile cold colors are representative of fast velocities.*

The scientists used the inversion method to investigate the structure of the crust and upper mantle beneath the Tarim and the Junggar sedimentary basins in central Asia, which include the location of the Chinese nuclear test site at Lop Nor. These basins are in a region of dramatic tectonic processes that have left their mark in the region's extreme variability in topography. The main features of the model are: (1) low velocities in the basins dominate the images at shallow depths because of the large amount of sediments found in the basins; (2) high lower crust and upper mantle velocities underneath the Tarim basin, which indicates an old, cold, and thick lithosphere that has not been greatly deformed; and (3) velocity images suggest differences in crustal and upper mantle structure between eastern and western Tarim. Improved knowledge of the shear velocity structure of these two sedimentary basins is necessary to understand the geodynamic evolution of these large, important tectonic structures. Moreover, the better the models are, the more accurately scientists can detect, locate, and identify small events, which are recorded only at regional distances, and therefore improve monitoring capabilities for the comprehensive Nuclear Test Ban Treaty.

Reference: "Joint Inversion of Surface Wave Velocity and Gravity Observations and its Application to Central Asian Basins Shear Velocity Structure", Journal of Geophysical Research 114, B02314 (2009), doi:10.1029/2007JB005157.

**Carbon Dioxide Sequestration System Model Estimates Project Costs**

EES-16 researchers are leading the development of a system-level model called $CO_2$-PENS (Predicting Engineered Natural Systems) to help understand the processes involved in sequestering carbon dioxide ($CO_2$) in underground reservoirs. The goal of building $CO_2$-PENS is to create a Performance Assessment/Risk Assessment tool to analyze hundreds of potential $CO_2$ sequestration sites across the USA. This project is part of a global effort to reduce global greenhouse gas concentrations and reduce the possibility of long-term damage to our environment.


*Figure: Cover of Environmental Science & Technology showing geologic sequestration of carbon dioxide superimposed on an atmospheric release. Artwork by Anthony Mancino, PADSTE.*

Work in EES spans a range of topics such as 1) numerical modeling of multiphase $CO_2$ flow and transport through porous rocks, 2) laboratory and numerical studies of the durability of cement in contact with $CO_2$, 3) field and numerical studies of how $CO_2$ leaking from below ground mixes in the atmosphere, 4) optimization of surface pipelines for transportation of $CO_2$, and 5) methods to detect $CO_2$ migration from potential reservoirs toward the surface. This partial list illustrates the many types of calculations involved in a model of the entire sequestration system. Individual process level models often must be abstracted or reduced in complexity to fit into the larger system framework, and EES and D divisions are collaborating to build large system-level simulators. The system level simulations must be run using a Monte Carlo approach to sample the ranges in parameter uncertainty associated with each physical process.

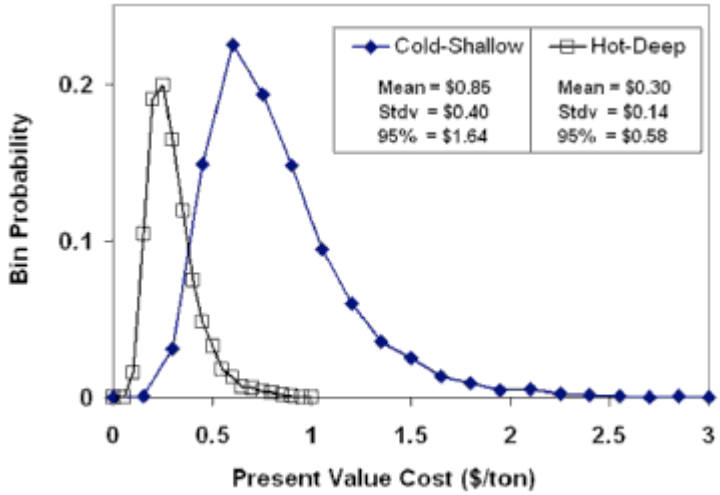


*Figure: Present value cost per ton associated with wells and local pipelines. Bin probability is the percent of the 5000 realizations found in a given bin used to create the histogram. The bin sizes are different for the two cases to allow the data to be plotted on the same figure.*

In a recently published paper featured on the cover of the journal *Environmental Science & Technology* and discussed in a news article entitled "Models of Carbon Storage Get Real", Philip Stauffer and EES-16 colleagues showed the usefulness of the system model approach for a prototype system involving the interaction between a process level injection module and an economic module. The injection module rapidly calculates how many wells will be required to inject a given mass of $CO_2$ into a specific reservoir considering uncertainty in permeability, porosity, and reservoir thickness. The economic module incorporates uncertainty in pipeline and drilling costs to estimate the final project costs. Fixed parameters that impact the results are the depth and temperature of the alternative target reservoirs.

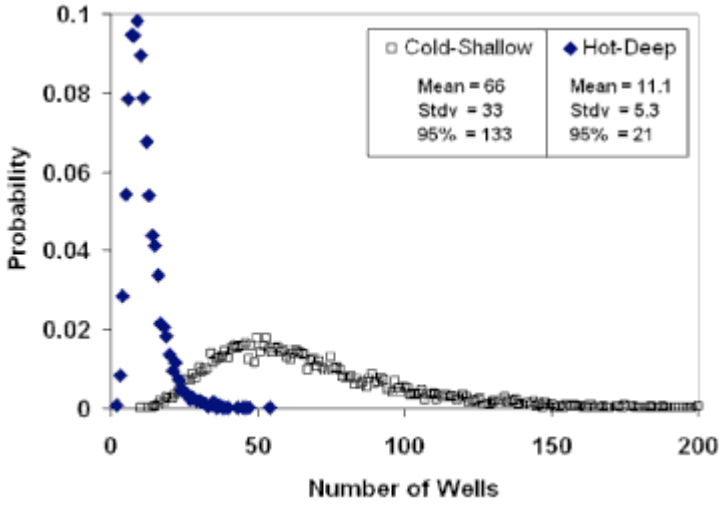


*Figure: Results for the two test cases showing the number of boreholes required to inject the $CO_2$ from a 1000 MW power plant. In each case 5000 realizations were run with values of permeability and porosity randomly chosen from the input parameter distributions.*

The figure above shows a comparison in the number of wells required to inject a fixed amount of $CO_2$ between a Hot-Deep (155 C and 3 km) case and a Cold-Shallow (35 C and 1 km) case. Because of variations in density and viscosity, the Hot-Deep case results in fewer required boreholes. This translates into a lower total cost per ton of $CO_2$ injected even though the deeper wells cost more to drill.

Authors include P.H. Stauffer, H.S. Viswanathan, and R.J. Pawar (all of EES-16); and G.D. Guthrie (formerly PADSTE-SPO, currently at NETL).

"A System Model for Geologic Sequestration of Carbon Dioxide" ***Environmental Science and Technology 43***, 565-570 (2009). The DOE Zero Emission Research and Technology (ZERT) Program supported this work.

**Oldest Hominid Skeleton Provides New Evidence for Human Evolution**

Discovery in Ethiopia of the oldest nearly intact skeleton of *Ardipithecus ramidus,* who lived 4.4 million years ago, is described in a special issue of the journal *Science* that includes 11 papers related to the discovery. An international research team has spent 17 years analyzing the fossils. LANL geologist Giday WoldeGabriel (EES-16), who led the field geology and laboratory studies to determine the age of the extremely fragile fossils, is a coauthor of two of the papers. This is the earliest skeleton known from the human branch of the primate family tree. The discovery reveals the biology of the first stage of human evolution better than anything seen to date and provides new insights about how hominids- the family of "great apes" comprising humans, chimpanzees, gorillas and orangutans- may have emerged from an ancestral ape.

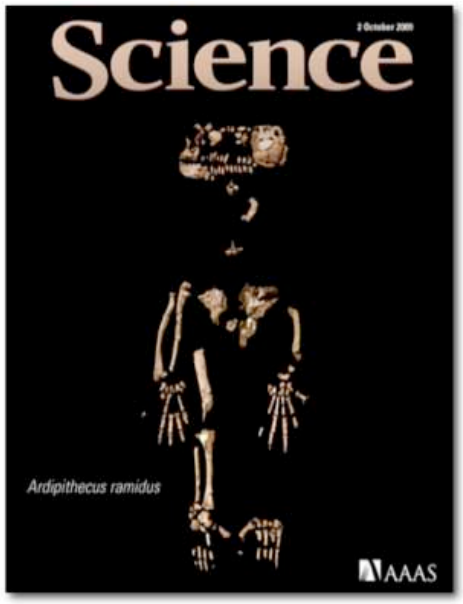


*Figure: Cover of the special issue of the journal Science, showing the oldest nearly intact skeleton of Ardipithecus ramidus.*

WoldeGabriel and collaborators used field and laboratory geological methods to determine the age of the extremely fragile fossils by painstakingly analyzing and dating the stratigraphic markers of ancient lavas, ashes, and sedimentary deposits in which the bones were discovered. The scientists were able to precisely characterize the environment in the hominids lived. The evidence indicates that *Ardipithecus ramidu* did not live in the open savanna that was once envisioned to be the predominant habitat of the earliest hominids, but rather in an environment that was humid and cooler than it is today, containing habitats ranging from woodland to forest patches. The woodland included fresh-water springs and small patches of fairly dense forest. Palm trees graced the forest edges, and grasslands extended perhaps many kilometers away. Other fossils associated with the hominids include fig and hackenberry trees, land snails, diverse birds, including owls, parrots, and peafowl; small mammals such as shrews, mice, and bats; and other animals such as porcupines, hyenas, bears, pigs, rhinos, elephants, giraffes, two kinds of monkey, and several different types of antelope.

*Figure: WoldeGabriel performs fieldwork in Ethiopia.*

"The Geological, Isotopic, Botanical, Invertebrate, and Lower Vertebrate Surroundings of *Ardipithecus ramidus*.", *Science* 326, 65 (2009), doi: 10.1126/science.1175817.

*"Ardipithecus ramidus* and the Paleobiology of Early Hominids", *Science* 326, 75 (2009), doi: 10.1126/science.1175802.

The Institute of Geophysics and Planetary Physics of the University of California at Los Alamos National Laboratory supported WoldeGabriel's work.

**Paul Johnson Coauthors Book on Nonlinear Mesoscopic Elasticity**

Nonlinear Mesoscopic Elasticity describes nonlinear behavior primarily in Earth materials-rock and unconsolidated materials such as sand. The book also includes some industrial materials that show how universal the nonlinear behaviors of granular media are. The book, a culmination of many years of research in this field by Johnson and Guyer, presents new tools and models in a systematic and thorough way. This comprehensive book is designed for anyone involved in non-destructive testing, civil engineering, and geophysics.

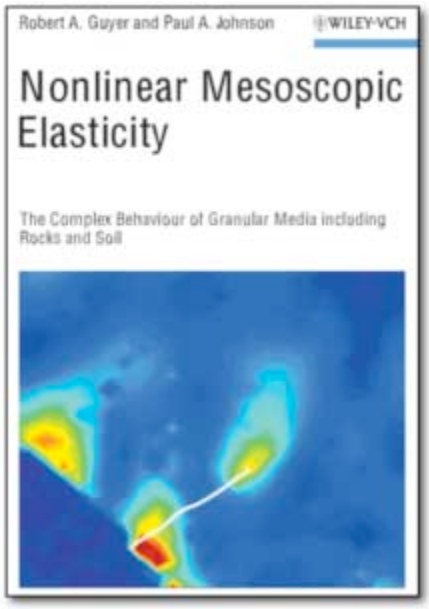


*Figure: Paul Johnson (EES-17) and coauthor Robert Guyer (University of Massachusetts - Amherst) discuss topical, practical uses for an improved understanding of the complex behavior of rocks and other materials.*

The DOE Office of Basic Energy Sciences and Laboratory Directed Research and Development (LDRD) supported Johnson's work.

**Tracer Experiments and Modeling Simulations through Unsaturated Tuff**

Yucca Mountain was studied extensively to determine whether it is a suitable site for a high-level nuclear waste repository. Much research has been conducted on the hydrologic and geochemical properties of the vadose and saturated zones surrounding Yucca Mountain. Experiments have been performed at the proposed waste storage horizon in the Exploratory Science Facility, but rocks below this level are difficult to access within Yucca Mountain. Therefore, the Busted Butte Unsaturated Zone Transport Test (UZTT) was designed to access exposures of the Topopah Spring Tuff and the Calico Hills Tuff, units stratigraphically correlative and mineralogically similar to the unsaturated rocks underlying the proposed repository.

Busted Butte is located at the Nevada Test Site, 8 km southeast of Yucca Mountain. The UZTT was initiated to explore the *in situ* behavior of solute and colloid movement through the tuff horizons that underlie the proposed repository. Specific issues of concern include the interaction of solute and colloid transport with heterogeneity and fractures, applicability of measured laboratory parameters to the field scale and site scale, and evaluation of numerical models for unsaturated transport in fractured tuff.

EES researchers Philip Stauffer, Jasper Vrugt, H. Jake Turin, Carl Gable, and Wendy Soll conducted a series of experimental and modeling tests using data from the Busted Butte Unsaturated Zone Transport Test.

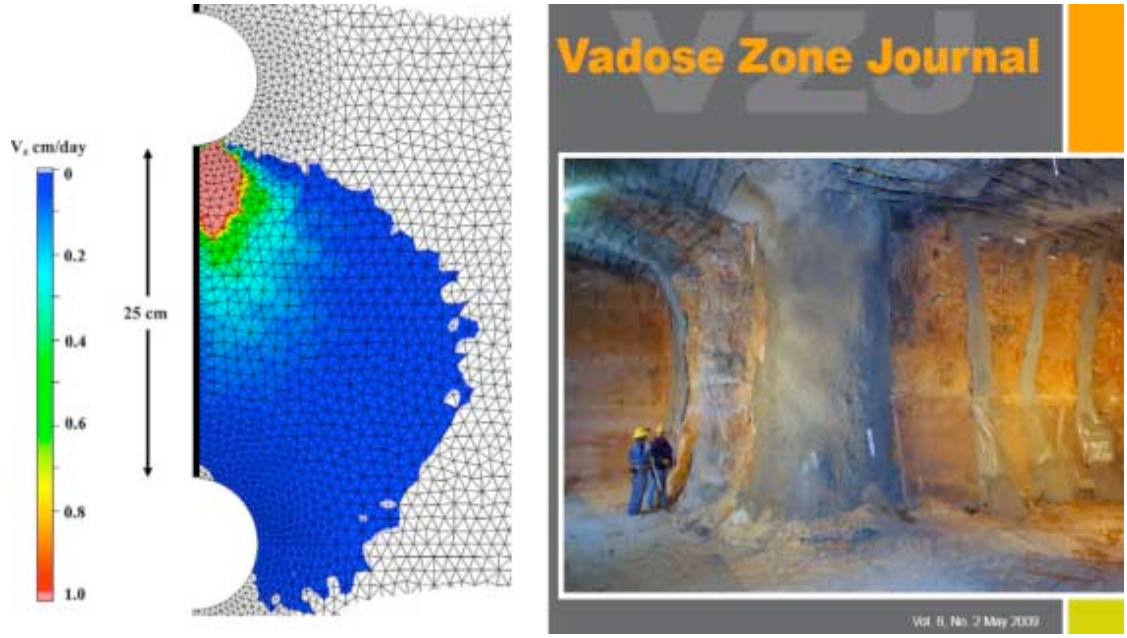


*Figure: Left - Magnitude of the vertical volumetric flux at the time of initial tracer breakthrough. Advection is dominant in the upper 10 cm while diffusion becomes dominant in the lower section of the tracer flow path. Right - Cover image for the Vadose Zone Journal showing the L-shaped alcove used to conduct the Busted Butte Unsaturated Zone Transport Test. Gilles Bussod (formerly of EES) led this interdisciplinary project.*

The scientists conducted a suite of reactive (e.g., lithium), nonreactive (bromide), and colloidal tracer experiments in a side alcove at the Test Facility. The researchers used the FEHM numerical simulator (finite element heat and mass transfer porous flow) populated with laboratory-measured hydrologic properties to verify that the conceptual model of the tracer test yielded a good fit to the tracer breakthrough data. They also employed search algorithms to find optimal parameter estimates in the conceptual model and to estimate their uncertainty. The FEHM model was run more than 50,000 times using parallel computing on a distributed computer cluster. The experimental and modeling results show that no observed breakthrough of colloids, low breakthroughs of lithium, and measured significant and rapid breakthrough of bromide.

The test captured both advective (transport of a substance in a fluid) and diffusive tracer transport. Measured hydraulic parameters from rock core samples provide a relatively accurate description of flow and transport at the scale and flow rates of the Busted Butte test. The data imply that one should be particularly careful in assigning values of the unsaturated subsurface flow and transport parameters without recourse to examining both parameter and model formulation uncertainty.

This paper is highlighted in the journal cover artwork and is further discussed in a News Article entitled "Unsaturated Zone Interest Group Overcomes Barriers to Advance Interdisciplinary Science" in the May 2009 edition of *CSA News*, the official magazine for members of the American Society of Agronomy, Crop Science Society of America, and Soil Science Society of America.

The DOE Civilian Radioactive Waste Management Program, Yucca Mountain Site Characterization Program Office supported the experimental design, data collection, and initial modeling. A LANL J. Robert Oppenheimer Fellowship supported J.A. Vrugt.

"Untangling Diffusion from Advection in Unsaturated Porous Media: Experimental Data, Modeling, and Parameter Uncertainty," *Vadose Zone Journal* 8, (2009), doi: 10.2136/vzj2008.0055.

**Understanding Arctic Temperature Change Amplification**

Understanding the past variability in Arctic temperatures is essential to assess the future melting of the Greenland ice sheet, Arctic sea ice, and Arctic permafrost. Models predict that the Arctic warms 2 to 3 times faster than the global mean.

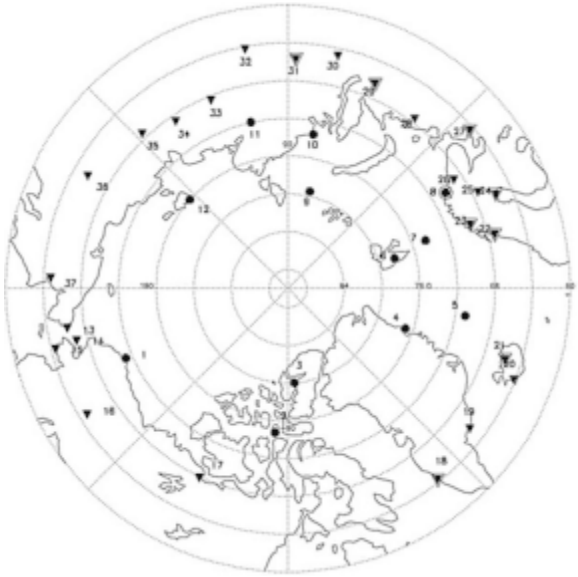

*Figure: Arctic - ~37 surface temperature monitoring stations from which data are used to reconstruct the Arctic temperature record from 1880.*

In a paper published in July 2009, Petr Chylek (ISR-2), Manvendra Dubey (EES-14), and collaborators at UK-Met Office, University of Washington, and Dalhousie University analyzed the century-long observational record of surface temperatures to quantify the warming in the Arctic relative to the global mean. They identified two distinct warming periods, 1910-1940 and 1970-2008, with respective Arctic warming rates that are 5.4 and 2 times larger than rates of global warming. The intervening period of 1940-1970 cooled at a rate about 9 times faster than the global cooling rate.

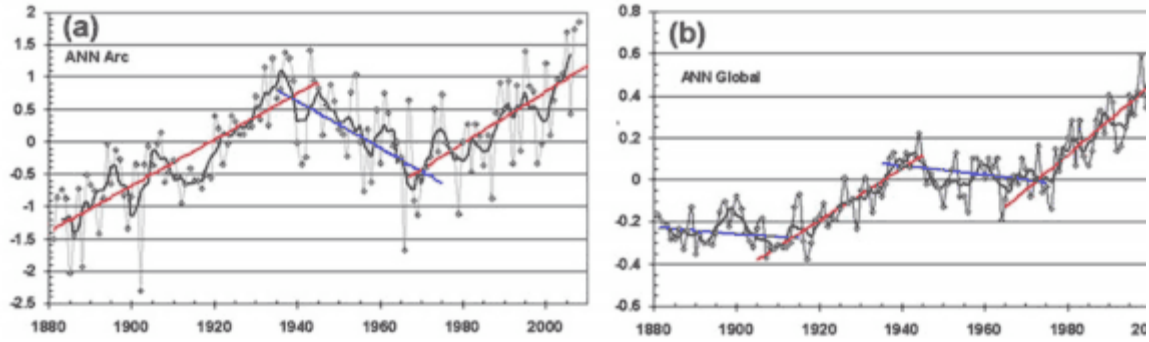

*Figure: Annual average temperature anomalies relative to the 1910-2008 average for the Arctic (left) and Earth (right). The heavy solid black line is a 5-year running mean. The solid colored lines are the linear regressed trends for the 3 distinct periods.*

The Arctic temperature changes are highly correlated with the Atlantic Multi-decadal Oscillation (AMO), suggesting that the Atlantic thermohaline circulation is linked to the Arctic temperature variability on multi-decade timescales. The scientists conclude that the ocean thermohaline circulation may be a greater factor than carbon dioxide and other greenhouse gases in influencing the Arctic climate. The observations confirm that the Arctic has warmed twice as fast as the world over the last 4 decades as simulated by coupled climate models.

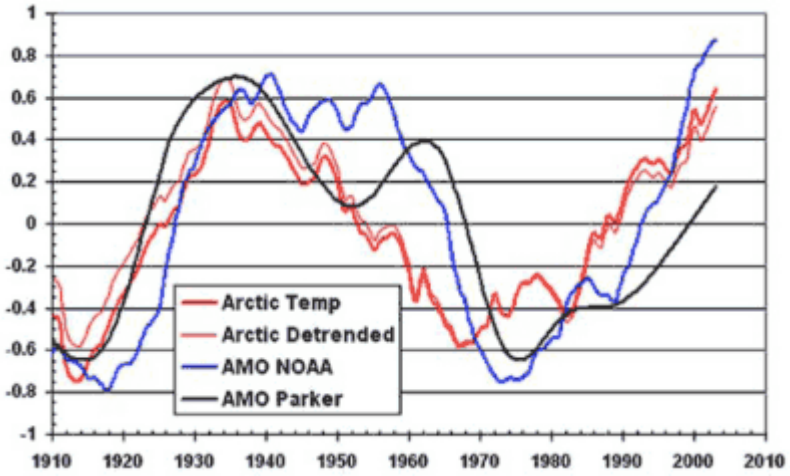


*Figure: The 11- year running average of Arctic temperature anomaly in K (red lines, detrended is thick red line) and the AMO index anomaly from NOAA (black) and UK Met Office (Blue).*

However, most models under-predict the rapid Arctic warming observed in the early part of the 20th century. This result suggests that there are physical processes in the climate system that are not yet fully understood and properly described by the current models. This problem should be resolved by ensuring that coupled-climate models reproduce the observed natural oscillations such as the AMO. This is critical to determine whether natural climate variability will make the Arctic more or less vulnerable to anthropogenic global warming that is projected to intensify in the near future.

"Arctic Air Temperature Change Amplification and the Atlantic Multidecadal Oscillation", *Geophysical Research Letters* 36, L14801 (2009), doi:10.1029/2009GL038777.

LANL Laboratory Directed Research and Development (LDRD) supported the LANL research.

**_Science_ Selects "Breakthrough" Article of the Year**

Each year, the journal *Science* selects the top 10 published scientific advances of the year. This year, *Science's* choice for the top Breakthrough of the Year is the reconstruction of the 4.4-million-year-old *Ardipithecus ramidus* skeleton and her environs, published in Science as a major series of 11 articles in October (Science, 2 October, pp. 60-106). Although some hominins (the family that includes humans and our ancestors) are even older, *Ardipithecus* is by far the most complete specimen of such antiquity. The work changes the way scientists think about early human evolution. The discoverers proposed that *Ardipithecus* was a new kind of hominin, who had an unusual anatomy unlike that of living apes or later hominins. *Ardipithecus* reveals the ancient anatomical changes that laid the foundation for upright walking. If so, our ancestors began walking upright while still living primarily in a woodland rather than in more open, grassy terrain, as once believed. The reconstruction represents the culmination of 15 years of highly collaborative research by an international team 47 scientists of diverse expertise, who made a

painstaking analysis of the 150,000 specimens of fossilized animals and plants. The eleven *Ardipithecus* papers, comprising 89 pages of text plus 295 pages of supporting online material, provide an enormous amount of data. *Time* magazine also selected the reconstruction of *Ardipithecus* as number one in the Top 10 Scientific Discoveries of 2009.


*Figure: L - Science cover depicting Ardipithecus ramidus, a possible human ancestor, inhabited then-wooded regions of Ethiopia 4.4 million years ago. Image © 2009, Jay Matternes. R - Cover of the special issue of the journal Science, showing the oldest nearly intact skeleton of Ardipithecus ramidus.*

LANL geologist Giday WoldeGabriel (EES-16), who led the field geology and laboratory studies to determine the age of the extremely fragile fossils, is a coauthor of two of the papers. WoldeGabriel and collaborators used field and laboratory geological methods to determine the age of the extremely fragile fossils by painstakingly analyzing and dating the stratigraphic markers of ancient lavas, ashes, and sedimentary deposits in which the bones were discovered. The scientists precisely characterized the environment in the hominids lived. The evidence indicates that *Ardipithecus ramidus* did not live in the open savanna that was once envisioned to be the predominant habitat of the earliest hominids, but rather in an environment that was humid and cooler than it is today, containing habitats ranging from woodland to forest patches. The woodland included fresh-water springs and small patches of fairly dense forest. Palm trees graced the forest edges, and grasslands extended perhaps many kilometers away. Other fossils associated with the hominids include fig and hackenberry trees, land snails, diverse birds, including owls, parrots, and peafowl; small mammals such as shrews, mice, and bats; and other animals such as porcupines, hyenas, bears, pigs, rhinos, elephants, giraffes, two kinds of monkey, and several different types of antelope.

*Figure: WoldeGabriel performs fieldwork in Ethiopia.*

The Institute of Geophysics and Planetary Physics of the University of California at Los Alamos National Laboratory (Gerald Geernaert, LANL IGPP Center Leader) supported WoldeGabriel's work.

"The Geological, Isotopic, Botanical, Invertebrate, and Lower Vertebrate Surroundings of *Ardipithecus ramidus*", *Science* 326, 65 (2009), doi: 10.1126/science.1175817

*"Ardipithecus ramidus* and the Paleobiology of Early Hominids", *Science* 326, 75 (2009), doi: 10.1126/science.1175802.

**Volcanic Hazard and Risk Assessment**

A book published by Cambridge University Press includes a chapter by Greg Valentine (formerly in EES, currently at State University of New York, Buffalo) and Frank Perry (EES-16) titled "Volcanic Risk Assessment at Yucca Mountain, NV, USA: Integration of Geophysics, Geology, and Modeling". The book, *Volcanic and Tectonic Hazard Assessment for Nuclear Facilities,* has 26 chapters describing methods and case studies of volcanic and tectonic hazard assessment for nuclear facilities around the world. The chapters describe multiple hazards that potentially impact nuclear power plants and nuclear waste repositories including seismic and volcanic hazards, tsunamis, tectonic uplift and subsidence, glacial rebound, erosion, sea-level rise and storm surge.

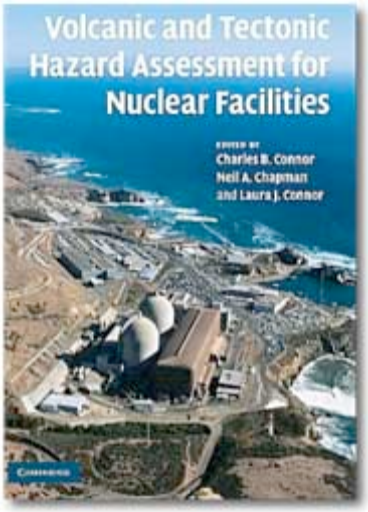


Assessing volcanic hazard at Yucca Mountain was an important component of DOE's license application in 2008 to the Nuclear Regulatory Commission because Yucca Mountain lies within a region that has experienced sporadic basaltic volcanism for the past several million years and as

recently as 80,000 years ago. Valentine and Perry describe the research conducted with other scientists in EES Division that resolved several key issues related to volcanic hazard and risk at Yucca Mountain. One issue was the number, age, and location of volcanic centers buried in the sedimentary basins that adjoin Yucca Mountain. These data were needed to determine the recurrence rate of volcanism in the Yucca Mountain region over the last several million years.

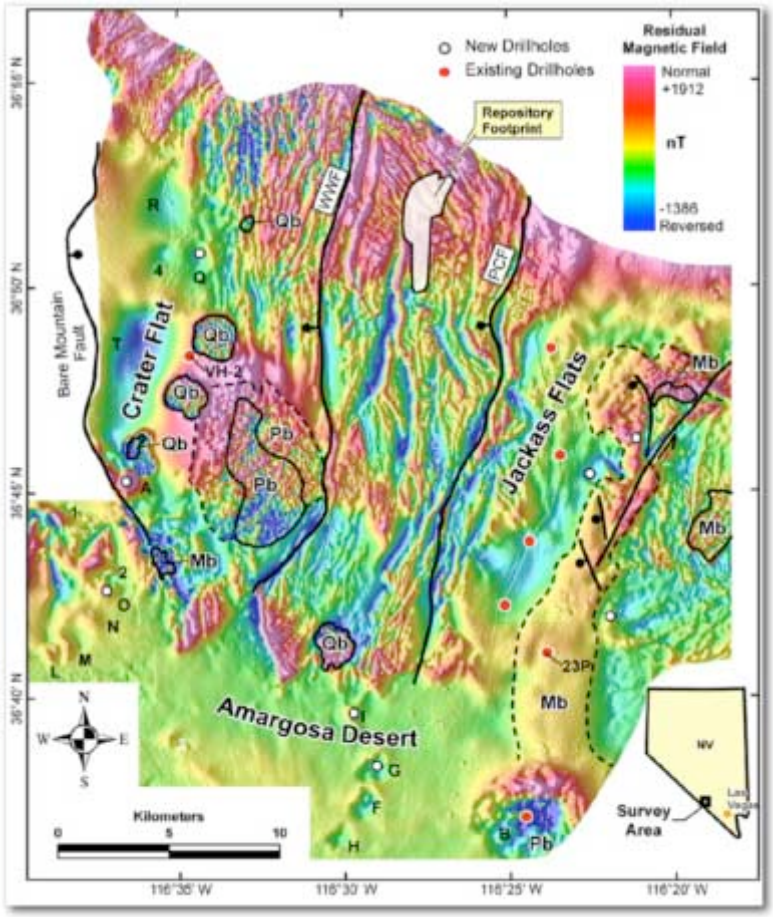


*Figure: Map showing area surveyed surrounding Yucca Mountain.*

A combined program of geophysics, drilling, geochronology, and geochemistry (above) showed that only a few buried volcanoes were less than five million years old and helped to resolve controversy concerning the volcanic recurrence rate in the region. Modeling studies described in the chapter resolved how waste packages would behave if magma intruded the repository drifts, and how contaminated volcanic ash would be distributed given the low probability event of a volcanic eruption intersecting the proposed high-level waste repository.

The DOE Office of Civilian Radioactive Waste Management (Bruce Robinson, LANL Program Manager) funded the work.

**Predicting the Fate of the Amazon Rainforest Under Changing Climate**

The likely fate of the Amazon rainforest under future hotter and drier climate regimes is the subject of a paper co-authored by Rosie Fisher (EES-14) in a special section of the *Proceedings of the National Academy of Sciences USA* devoted to "Tipping Elements in Earth Systems." The paper builds on her previous work on the resilience of Amazonian forests to drought stress.

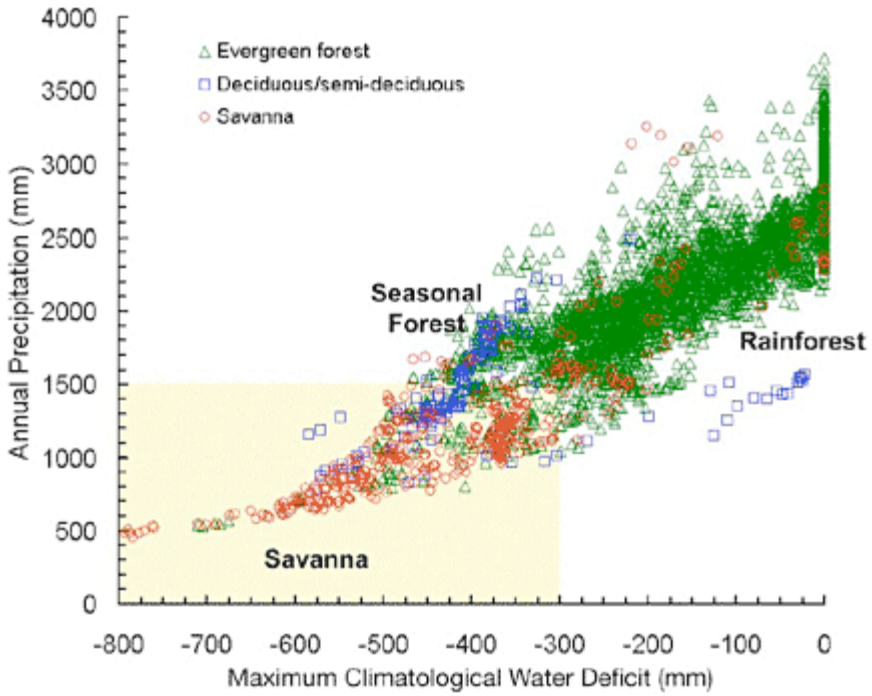


*Figure: The relationship between vegetation type and rainfall regime. Rainfall regime is derived from Tropic Rainfall Monitoring Missions for the period 1998-2006. The suggested savanna zone is shaded (maximum climatological water deficit less than -300 mm, annual precipitation less than 1500 mm).*

The research assesses evidence, including 19 global climate model scenarios, that 21st century climate change may cause widespread "die-back" or degradation of the Amazon forest. The analysis suggests that Eastern Amazonia is likely to shift towards a climate more appropriate for savanna over the 21st century, but the speed of the shift might be modified by human intervention to reduce fire and deforestation rates. Thus, the loss of the Amazon in the 21st century should not yet be considered as inevitable.

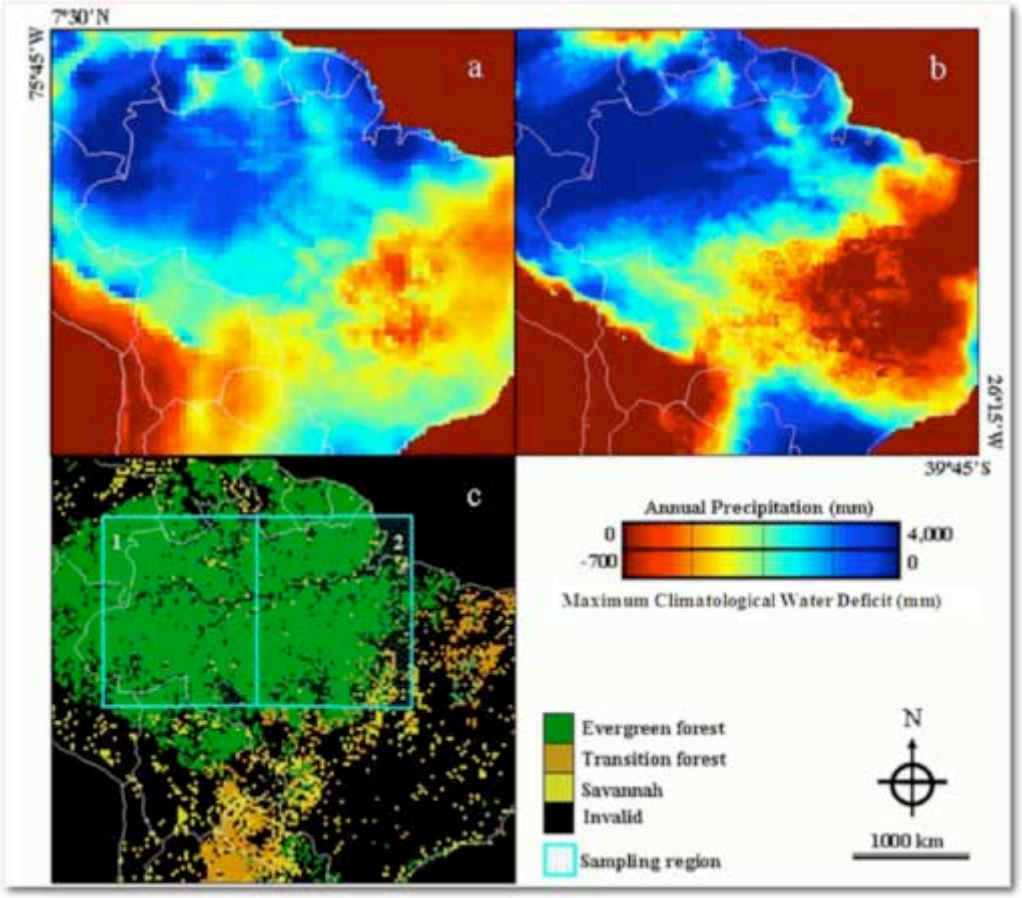


*Figure: The variation of rainfall regime and vegetation type across Amazonia, which forms the basis of the biogeographical analysis. Maps of annual precipitation (a) and climatological water deficit (b), derived for the period 1998-2007, from the Tropical Rainfall Monitoring Missions. (c) Map of vegetation cover in 2000.*

The paper was also cited in *The Copenhagen Diagnosis,* which was published this month. The book documents the key findings in climate change science since the publication of the landmark Intergovernmental Panel on Climate Change (IPCC) Fourth Assessment Report in 2007, and serves as an interim evaluation of the evolving science midway through an IPCC cycle.

"Exploring the likelihood and mechanism of a climate-change-induced dieback of the Amazon rainforest", *Proceedings of the National Academy of Science USA* 106, 20610 (2009), doi:10.1073/pnas.0804619106.

*The Copenhagen Diagnosis,* University of New South Wales (2009), ISBN: [978-0-9807316-0-6].

**Model Developed to Understand Regional Aquifer Beneath LANL**

Understanding and predicting groundwater flow and contaminant transport at large spatial scales in subsurface systems requires integrating knowledge of aquifer heterogeneity and field-scale parameterizations. Zhenxue Dai, Elizabeth Keating, Carl Gable, Daniel Levitt (EES-16); Jeff Heikoop (EES-14); and Ardyth Simmons (PROJMGMT) developed a methodology to understand heterogeneity and parameter scaling in the regional aquifer beneath the LANL site.

Based on the regional hydrogeology and the stratigraphy beneath the Pajarito Plateau, the scientists built a site-scale groundwater model with more than 20 stratified hydrologic units.

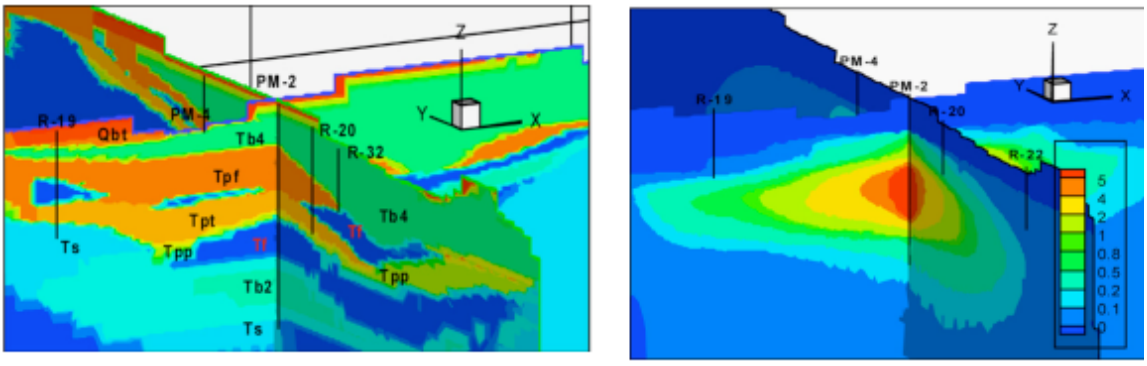


*Figure: (a) Outline of the hydrologic units around PM-2 pumping well and (b) the simulated drawdown distribution of the PM-2 pumping test at 25 days (PM-2 well is located at the center of two cross sections, drawdown unit is in meters).*

Their stepwise inverse method couples observation data from different sources and spatial scales, including single-well and multiple-well pumping tests and regional aquifer monitoring data. The model estimates permeabilities for the hydrologic units (Figure 2). The joint inversion offers a reasonable fit to all data sets, indicating the usefulness of the model to simulate the complex heterogeneity of the aquifer system beneath the Pajarito Plateau.

The DOE Environmental Remediation program supported the work.

"Stepwise Inversion of a Groundwater Flow Model with Multi-scale Observation Data", *Hydrogeology Journal,* doi: 10.1007/s10040-009-0543-y, November, 2009.

**Fresh Paleowater on the Atlantic Continental Shelf Could Provide Water for Megacities**

Freshwater springs are found along the Atlantic coastal shelves of North America and Europe at depths of several hundred meters below sea level and several hundred kilometers offshore. In some areas (the southern U.S), springs emanate from coherent aquifers that are recharged high enough above sea level to provide the gravitational potential to push the fresh water out into the denser saltwater. In other areas, the fresh water may have been trapped during glacial cycles when sea level was considerably lower.

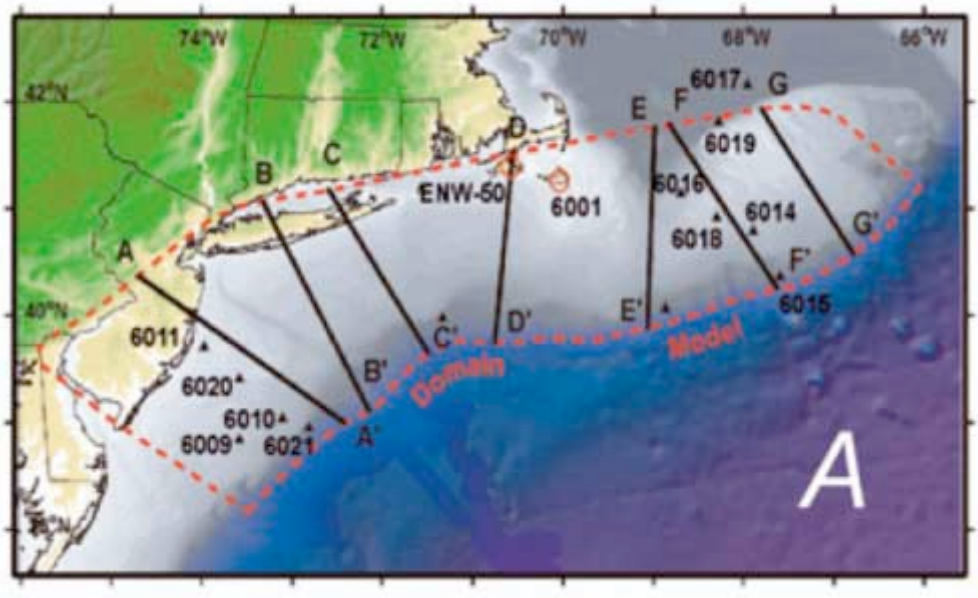

*Figure: (A) Areal footprint of the three-dimensional paleohydrologic model (dashed line) along the Atlantic continental shelf in New England and location of cross sections and wells.*

Carl Gable (EES-16) and collaborators (Iowa State University, New Mexico Tech, Indiana University, U.S. Geological Survey, Rice University, VU University Amsterdam, and Woods Hole Oceanographic Institution) explored the mechanism of formation and resource potential of the paleowater.

The scientists used high-resolution paleohydrologic models of groundwater flow, heat and solute transport, ice sheet loading, and sea level fluctuations for the continental shelf from New Jersey to Maine over the last 2 million years. The models suggest that extensive recharging occurred beneath Pleistocene ice sheets, which extended out onto the shelves or along submarine canyons. The researchers estimate that some submarine aquifers off New England may contain as much as 10,000 $km^3$ of fresh water, and there may be as much as 300,000 $km^3$ of trapped fresh water globally. The offshore fresh water is a valuable, although nonrenewable, resource for coastal megacities faced with growing water shortages.

The research was highlighted as an Editor's choice in the journal *Science* 326, 1164 (2009).

The University of Indiana supported the LANL work.

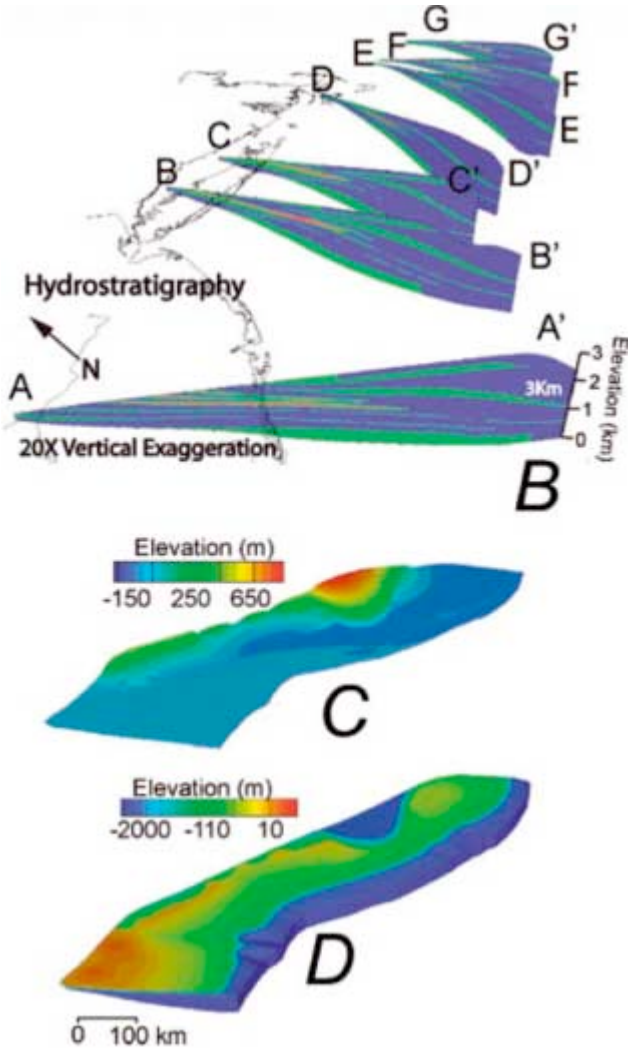


*Figure: (B) Cross-sectional transects depicting hydrostratigraphic units represented in the three-dimensional model: silt/clay (blue), fine sand (red), and medium to coarse sand (green) units.*

*Note that the shallow sands crop out in submarine canyons. Imposed surface hydraulic heads (C) and topography/bathymetry of continental shelf (D) during the last glacial maximum, 21,000 years before present. Areas of high imposed heads (> 250 m) delineate the approximate location of the Laurentide ice sheet.*

"Origin and Extent of Fresh Paleowaters on the Atlantic Continental Shelf, USA", *Groundwater* 10.1111/j.1745-6584.2009.00627.x (2009).

**Investigation of Nonvolcanic Seismic Tremors**

Non-volcanic tremor (NVT) and slow slip are unusually slow earthquakes that occur in diverse tectonic environments. They appear to have the same mechanism as ordinary earthquakes, but differ in their source location and moment-duration scaling. Ordinary earthquakes grow explosively in size with increasing duration, but slow earthquakes grow at a constant rate. The hazard implications of tremor and slow-slip are significant. They are typically found on the deep extension of faults, just below the region of the fault that produces the more familiar, and dangerous, "ordinary" earthquakes. Thus, the slip from these slow events could load, or even trigger, large earthquakes in the shallower portion of the fault zone. Studying triggered NVT helps to map the depth of the locked zones of faults associated with high seismic risk. The success of mapping depends on precisely locating the depth of tremor.

Monica Maceira and Carene Larmat (EES-17) and colleagues J. Rubinstein and E. Roeloffs (U.S. Geological Survey) convened a topical session to address NVT and slow slip during the Annual Meeting of the Geological Society of America, held at Portland, OR. The session, "Slow Slip and Non-volcanic Seismic Tremor in Cascadia and Beyond: Observations, Models, and Hazard Implications", was comprised of presentations of critical observational and modeling constraints that bear on all aspects of episodic non-volcanic tremor and slow slip events.

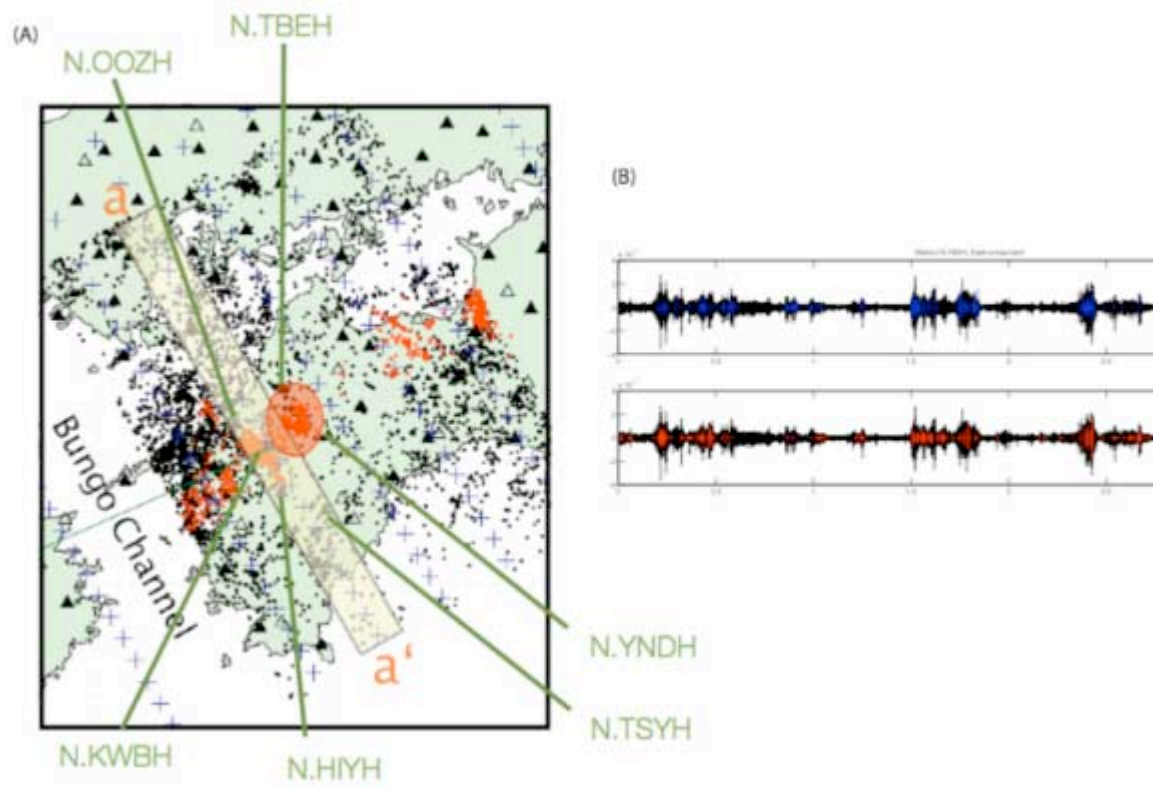


*Figure: (A) Map of southwest Japan with regular earthquakes (black dots) and previously identified LFEs (red dots). The big red shadow eclipse encloses the 188 LFEs previously identified for the 1-hour tremor signal. Black triangles represent JMA stations. Green lines point to*

*stations used for this study. (B) An hour-long period of tremor recorded at station N.TBEH, east component. Previously identified LFEs are indicated in blue (top); newly identified LFEs by this study are shown in red (bottom).*

Maceira presented NVT related research with collaborators C. Rowe (EES-17) and G. Beroza (Stanford University) in "Identification of Low-frequency Earthquakes on Non-volcanic Tremor Validated with the Subspace Detector Method". NVT episodes may be comprised of a sequence of repeating low-frequency earthquakes (LFEs). A previous researcher identified 188 LFEs in a one-hour episode of tremors recorded at borehole stations belonging to the Japan Meteorological Agency (JMA). Maceira and colleagues built upon this work by searching for additional LFEs within the data stream. They used a subspace detection method, which takes a matrix of master event waveforms and builds a set of basis vectors to reproduce the master waveforms. Operating on the assumption that any waveform from the same source region and with a similar source mechanism can be characterized as a linear combination of their basis vectors, the scientists searched for additional LFEs. They tested the method using an hour-long segment of continuous seismic data recorded at JMA stations. Application of the subspace detector to events identified by two different decision methods confirmed that the discrete LFEs occurring during the hour of tremor are restricted to the previously identified portions of the traces. The researchers detected some additional events that fill in temporal gasps in the LFE-rich portions of the trace (above figure). The most striking result of the results is the clearly defined changes in linearity and polarization exhibited in the waveforms. If LFEs are assumed to arise from a relatively consistent source region and have a fairly consistent mechanism, then the authors cannot accept the hypothesis that the entire waveform section can be explained as overlapping, repeating LFEs. The Institute of Geophysics and Planetary Physics (IGPP) program and DOE NNSA support the work.

Larmat (EES-17) presented research with colleagues R.A. Guyer and P.A. Johnson (EES-17) in "Location and Characterization of California Nonvolcanic Tremor using Time Reversal, Investigation of Different Imaging Fields". Non-volcanic tremors lack distinct sharp timing features, making it difficult to locate with classical triangulation approaches. Time Reversal (TR) is a promising method as it only requires having synchronized recorded waveforms. TR is based on the inherent invariance of the wave equation to the inversion of the time-axis. The scientists conducted a TR location study with a realistic receiver set for the volume surrounding a segment of the San Andreas fault in California and a 3D velocity mode (above). The key to successfully locating NVT is application of suitable imaging fields, such as the wave divergence, curl, and energy current. What is seen on the surface (3c above) is different from what is seen at source depth (3d above).

LANL Laboratory Directed Research and Development (LDRD) supports the work.

"Tremor source location using Time Reversal: Selecting the Appropriate Imaging Field", *Geophysical Research Letters* Volume: 36 Article Number: L22304 Published: 2009 , http://www.agu.org/journals/gl/papersinprest.shtml#id2009GL040099.

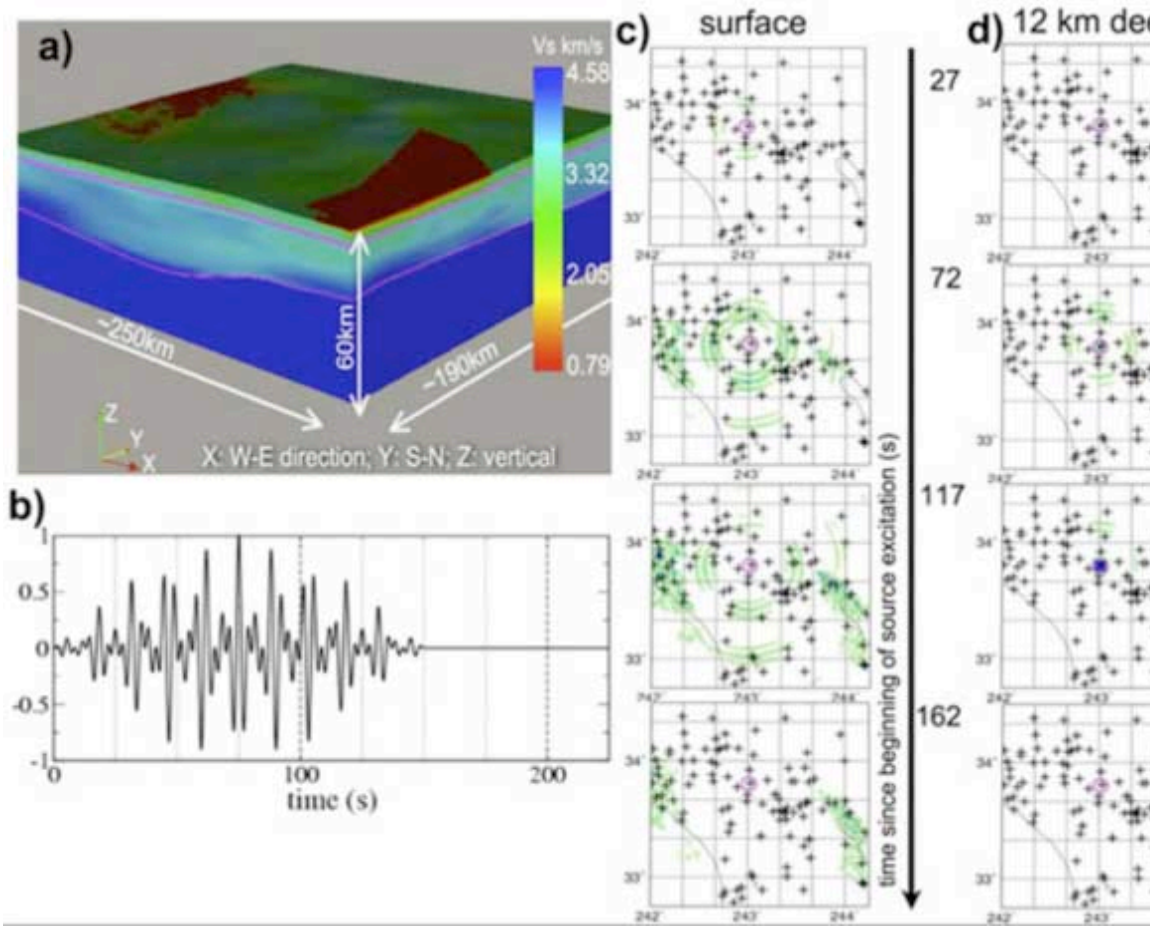


*Figure: (a) The 3D velocity model of the study volume, centered on the San Jacinto segment of the San Andreas Fault; co-ordinate system is at the lower left. (b) Long-lasting source time function applied with an horizontal strike-slip mechanism for the source. (c) and (d) Snapshots of the norm of the displacement field (b) at the surface, (c) at source depth, 12 km. Note the accumulation of seismic energy on the surface in the two low velocity zones [shown in yellow in (a)] corresponding to sedimentary basins on the east and west edges of the study volume.*

**First Documentation that Vegetation Mortality on all Six Vegetated Continents Increases with Climate Change**

Nate McDowell (EES-14) and collaborators have two papers in press regarding climate impacts on vegetation survival and mortality. LANL Laboratory Directed Research and Development, DOE-Office of Biological and Environmental Research, and the Institute of Geophysics and Interplanetary Sciences funded the LANL component of the work.

*Figure: Low-elevation ponderosa pine trees that died in 2002-2003.*

The first paper describes the results of their study in Bandelier National Monument, where the lower elevation treeline of ponderosa pine trees moved uphill by 200 meters in the 2002 drought. The scientists found evidence in support of McDowell's carbon starvation theory, which hypothesizes that drought intolerant species do not die of hydraulic failure (drying out), but rather, they die from the avoidance of hydraulic failure through stomatal closure and hence negligible photosynthetic uptake of carbon. (Stomata are tiny pores on the surfaces of leaves that permit the exchange of gases between the atmosphere and the inside of the leaf.) Thus, the researchers conclude that chronic water stress predisposed low-elevation trees to mortality during drought via constrained gas exchange. Continued intensification of drought in mid-latitude regions may drive increased mortality and ecotone shifts in temperate forests and woodlands.

*Figure: Satellite map of North America, with documented drought-induced mortality localities indicated with numbers. Inset photo(s) of forest mortality. Top photo: Aerial view showing severe mortality of aspen (Populus tremuloides) in the parkland zone of Alberta, Canada; 2004, by Michael Michaelian. Lower photo: Pinus ponderosa die-off, Jemez Mountains, NM, USA; 2006, by Craig D. Allen.*

The surviving understory of *Juniperus monosperma* is typical of transition to woodland. The second paper describes the first ever documentation that vegetation mortality on all six vegetated continents and across all biomes is increasing with climate change. This paper is an enormous step forward in demonstrating that climate change is driving a global-scale response of vegetation mortality.

"Growth, Carbon Isotope Discrimination, and Mortality Across a Ponderosa Pine Elevation Transect", *Global Change Biology,* Volume: 16 Issue: 1 Pages: 399-415 Published: 2010 doi: 10.1111/j.1365-2486.2009.01994.x

"Forest flora turnover with climate change in the Mediterranean region: A case study in Southeastern France ", *Forest Ecology and Management,* Volume 258, Supplement 1, 14 December 2009*, Pages S56-S63* doi:10.1016/j.foreco.2009.09.001,

**Chlorine Isotopic Signatures Distinguish Natural and Anthropogenic Perchlorate in Groundwater**

Perchlorate ($ClO_4^-$) is found in the environment from natural atmospheric reactions and synthetic products used in military, aerospace, and industrial applications. In addition, nitrate-enriched salt deposits of the Atacama Desert (Chile) containing high concentrations of natural $ClO_4$- are exported worldwide for agricultural use as fertilizer. The widespread environmental introduction of synthetic and agricultural ClO4- has contaminated many municipal water supplies and can cause risk to human health.

*Figure: Perchlorate collection from an artesian well feeding San Antonio Creek in Valle Toledo. Photo - Kim Granzow.*

Jeff Heikoop (EES-14/LANL Water Stewardship Project) and collaborators investigated chlorine isotopic signatures as a tracer of $ClO_4^-$ sources. The isotopic signatures are composed of the relative amounts of chlorine isotopes in $ClO_4^-$. The scientists found that desert soil and groundwater samples from the southwestern U.S. (including uncontaminated sites in the Jemez Mountains and Pajarito Plateau) contain ClO4- with a high abundance of the radioactive isotope chlorine-36 ($^{36}Cl$), compared with those from the Atacama Desert and synthetic $ClO_4^-$ products. The isotopic signatures distinguish among anthropogenic sources of $ClO_4^-$, natural $ClO_4^-$ native to the Southwest, and $ClO_4^-$ from the Atacama Desert. The results may have forensic applications to determine the sources of $ClO_4^-$ in water supplies and foodstuffs. At LANL, these results will assist scientists to determine if $ClO_4^-$ in groundwater at concentrations similar to accepted background levels is natural, anthropogenic, or a mixture. This information is critical for investigating the nature and extent of $ClO_4^-$contamination in groundwater.

Collaborating institutions include the University of Illinois - Chicago, Purdue University, United States Geological Survey, Oak Ridge National Laboratory, Texas Tech University, Shaw Environmental Inc., and the New Mexico Environmental Department.

The DOE Environmental Management Program supported the LANL work.

"Chlorine-36 as a Tracer of Perchlorate Origin", Environmental Science and Technology 43, 6934 (2009), doi: 10.1021/es9012195.

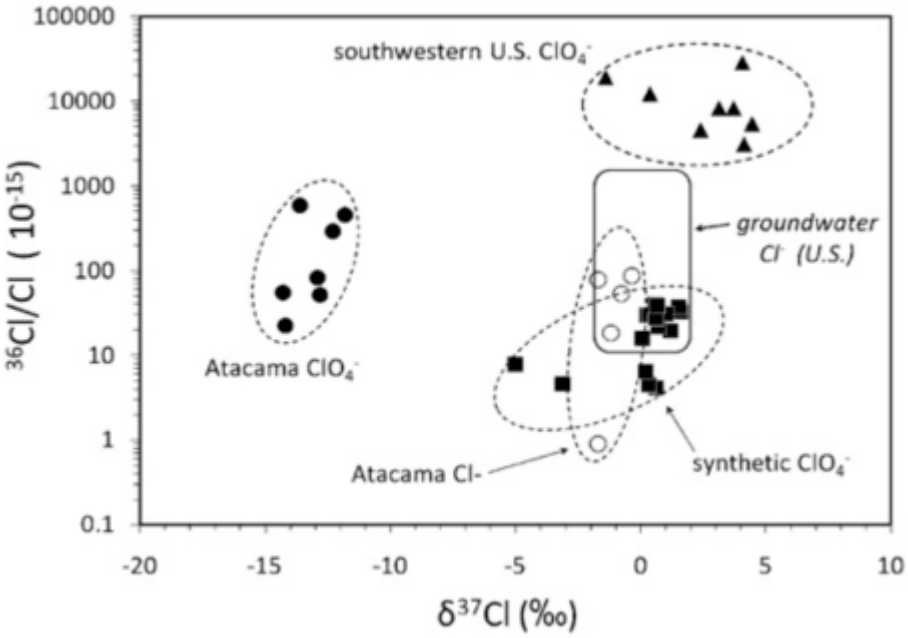


*Figure: $^{36}$Cl/Cl (atom ratio) vs. δ3$^{37}$Cl ($^0/_{00}$) in representative samples of synthetic $ClO_4^-$ reagents and products; natural $ClO_4^-$ and $Cl^-$ extracted from soil and groundwater from the Atacama Desert, Chile; and natural $ClO_4^-$ extracted from groundwater and soil from the southwestern U.S. Sizes of symbols exceed analytical errors. Delineated square area shows ranges of $^{36}$Cl/Cl ratios and δ$^{37}$Cl values for $Cl^-$ in U.S. groundwater.*

**Neutron Diffraction Studies of Jarosite**

Jarosite, a hydrous sulfate mineral [$KFe_3(SO_4)_2(OH)_6$], is of interest for its geological and industrial applications. It occurs in acid mine drainage environments as a weathering product of sulfide ore deposits and precipitates in epithermal environments and hot springs associated with volcanic activity. Jarosite is used as an iron-impurity extractor from zinc sulfide ores in the zinc industry and has been also proposed as a potential host for immobilization of radioactive fission products and toxic heavy metals. The detection of jarosite by the Mars Exploration Rover Mössbauer spectrometer has been interpreted as a strong evidence for the existence of water (and possibly life) on ancient Mars. This discovery has spurred interest in the stability and structural behavior of jarosite and related phases at various temperature, pressure, and aqueous conditions.

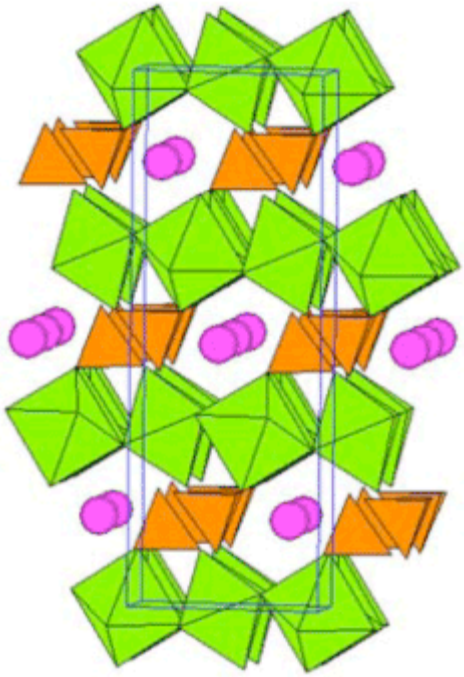

*Figure: Crystal structure of jarosite, [$KFe_3(SO_4)_2(OH)_6$]. Tetrahedra represent [$SO_4$] units, octahedra represent [$Fe(O,OH)_6$] units, and blue lines outline the unit. The c-axis of the structure is vertical.*

Hongwu Xu and Don Hickmott (EES-14), and Yusheng Zhao, Sven Vogel, Luke Daemen and Monika Hartl (LANSCE-LC) employed the time-of-flight neutron facility at the Lujan Neutron Scattering Center of LANSCE to investigate the structure and stability of a deuterated jarosite at temperatures up to 650 K. Since the scattering power of neutrons does not vary with the number of electrons in an element (as it does for X-rays), neutron scattering is much more sensitive to the positions of light elements (especially hydrogen and its isotopes) and is thus a powerful technique for studying hydrogen-bearing minerals/materials. Structural analysis of jarosite reveals that with increasing temperature, its c dimension expands at a rate approximately 10 times greater than that for a. This anisotropy of thermal expansion is due to rapid increase in the thickness of the (001) sheet of [$Fe(O,OH)_6$] octahedra and [$SO_4$] tetrahedra with increasing temperature. On heating, the hydrogen bonds through which the (001) octahedral-tetrahedral sheets are held together become weakened. On further heating to 575 K, jarosite starts to decompose into nanocrystalline yavapaiite and hematite, a direct result of the breaking of the hydrogen bonds that hold the jarosite structure together.

This study has for the first time unraveled the atomistic mechanisms of thermal expansion and decomposition of jarosite and provided important insights into its further applications. These results should be useful in evaluating any potential high-temperature applications (industrial and geological). For example, as jarosite starts to decompose at 575 K, it may not be suitable for wasteforms that are required to be stable at higher temperature. With regard to jarosite on Mars, this means it did not experience temperatures higher than 575 K in its history. Otherwise it would not exist now.

This work benefited from the use of the Lujan Neutron Scattering Center at LANSCE, which is funded by the DOE Office of Basic Energy Sciences.

"Thermal Expansion and Decomposition of Jarosite: A High-temperature Neutron Diffraction Study," *Physics and Chemistry of Minerals* Page 8 (doi: 10.1007/s00269-009-0311-5).

**Role of Seismic Stimulation on the Mobilization of Colloidal Particles**

Naturally occurring seismic events and artificially generated low-frequency (1 to 500 Hz) elastic waves can modify the production rates of oil and water wells, sometimes increasing and sometimes decreasing production. The decreases in production are of particular concern, especially when artificially generated elastic waves are applied as a method for enhanced oil recovery.

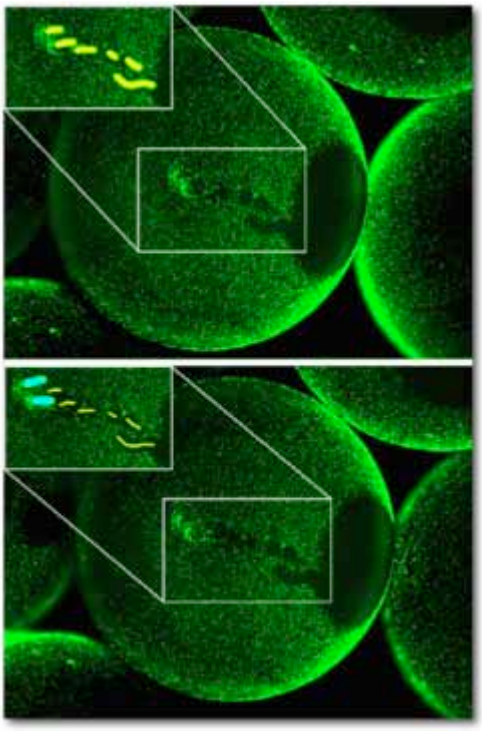

*Figure: Fluorescent images (50x magnification) of glass beads coated with fluorescent polystyrene microspheres after continuous loading followed by flushing with ultrapure water. The images captured before (top) and after (bottom) an episode of low-frequency flow oscillations provide evidence of the beads scraping against the cell wall during oscillations, as well as the piling up of particles in front of the point of contact. The insets highlight the locations of the paths scraped clear. Yellow marks indicate areas scraped before the top image was captured, and blue marks in the bottom image show new areas scraped after the top image was captured.*

Many applications including oil recovery, subsurface transport of contaminants, leakage of carbon dioxide geologic sequestration reservoirs, and remediation of contaminated aquifers could be altered as a result of this effect. The exact conditions that result in these changes remain unknown. Although the underlying environment is complex, the observed increase in water well turbidity after natural seismic events suggests the existence of a mechanism that can affect both the subsurface flow paths and the mobilization of in situ colloidal particles. The distribution and mobility of colloids would have major impacts on mass transport in any porous system. For example, migrating fines are known to clog some pore throats of porous networks under appropriate conditions. If the enhanced liberation of colloids could be understood quantitatively, then the underlying mechanisms might be utilized in developing new techniques for enhanced oil recovery and subsurface remediation.

Richard Beckham, Amr I. Abdel-Fattah, and Sowmitri Tarimala (EES-14); Peter Roberts (EES-17); and Reem Ibrahim (ENV-RRO) examined the macroscopic and microscopic effects of low-frequency dynamic stress stimulations on the release of colloidal particles from an analog granular core representing an infinitesimal section along the propagation paths of an elastic wave.

Their work showed, for the first time, that grinding of the grains causes physical displacement of the adsorbed colloidal particles, leading to their release. The intergranular grinding occurs in two modes: 1) It can involve only slight rubbing and grinding of pairs of grains throughout the entire column, which is observed at all levels of stimulation. The slight grinding mode results in a continuous release of microparticles from the column. 2) The other mode, which is observed only during higher levels of stimulation, involves numerous grains participating in a circulation cell during compaction of the media. The circulation cell mode causes spikes in the column's effluent colloid concentration at regular intervals. Although the experiments were performed in an idealized system (1-millimeter glass beads and 2-micron polystyrene colloids in de-ionized water), the conclusions also apply to irregularly shaped sand and consolidated sandstone, as well as adsorbed non-aqueous phase organic liquids and naturally occurring colloids.

Optical microscopy observations of the beads during low-frequency oscillations reveal that individual beads rotate, rubbing against each other and scraping away portions of the adsorbed microparticles. The release mechanisms appear to be associated with the compaction and relaxation of the granular material that result in the scraping of the grain surfaces, thereby mechanically displacing the adsorbed microparticles. These results support the theory that mechanical interactions between porous matrix grains are important mechanisms in flow path alteration and the mobilization of naturally occurring colloidal particles during elastic wave stimulation. This study supports the hypothesis that the changes in oil and water well production often observed during and after seismic events may be due in part to the release of natural colloids. This can cause either beneficial or harmful effects on formation permeability, depending on whether the released particles are expelled from the porous matrix or cause subsequent downstream fouling of flow pathways. These results also point to both continuous and discrete releases of colloidal particles, perhaps because of circulation cells within the packing material. The results of this study suggest that any event (seismic or otherwise) resulting in the compaction of an oil-bearing formation, including a reduction in pore pressure due to oil recovery; may reduce the production rate if the formation has a low permeability and a high natural colloid concentration. These results are critical to stimulated enhanced oil recovery, contaminant transport, and site remediation applications.

*Mobilization of Colloidal Particles by Low-Frequency Dynamic Stress Stimulation, Langmuir 26, 19 (2010); doi: 10.1021/la900890n.*

The DOE Basic Energy Sciences - Geophysics Program funded the research (David Janecky, LANL Program Manager).

**Giday WoldeGabriel Co-edits Book on Geological Context of Early Hominids**

Giday WoldeGabriel of EES-16 and Yohannes Haile-Selassie of the Cleveland Museum of Natural History co-edited and wrote chapters for the book, *Ardipithecus kadabba: Late Miocene Evidence from the Middle Awash, Ethiopia.* The University of California Press published the book in 2009.

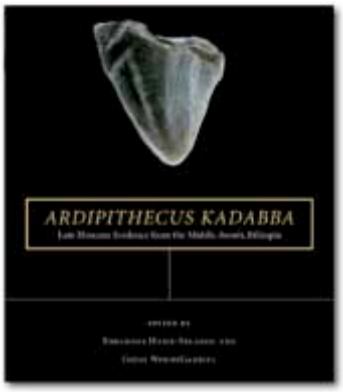


This is the second book in a series of seven volumes dedicated to the geological and paleontological investigations and fossil discoveries made in the Afar region of Ethiopia by the Middle Awash Project. WoldeGabriel, Professor Tim White (University of California - Berkeley), and Berhane Asfaw (Rift Valley Research Service, Ethiopia) co-led the international research team. This book contains the definitive description of the geological context and paleoenvironment of the earliest complete skeleton of the hominid *Ardipithecus kadabba.*

This research describes the Middle Awash geology and the late Miocene animal assemblages recovered from sediments firmly dated to between 5.2 and 5.8 million years ago. Compared to other assemblages of similar age, the Middle Awash record is unparalleled in taxonomic diversity, composed of 2,760 specimens representing at least 65 mammalian genera. This comprehensive evaluation of the vertebrates from the end of the Miocene in Africa provides detailed morphological and taxonomic descriptions of dozens of taxa, including species new to science. It also incorporates results from analyses of paleoenvironment, paleobiogeography, biochronology, and faunal turnover around the Pliocene-Miocene boundary (5.3 million years ago). These analyses open a new window on the evolution of mammals, African fauna, and its environments.

The journal *Science* selected the discovery and reconstruction of *Ardipithecus kadabba* and its environs as the top scientific breakthrough of the year.

The Institute of Geophysics and Planetary Physics of the University of California at Los Alamos National Laboratory (Gerald Geernaert, LANL IGPP Center Leader) supported WoldeGabriel's work. WoldeGabriel is an author of the following chapters of the book:

- Haile-Selassie, Y. and WoldeGabriel, G., "Introduction", pp. 1-26.
- WoldeGabriel, G., Hart, W. K., Renne, P. R., Haile-Selassie, Y., and White, T., "Stratigraphy of the Adu-Asa Formation", pp. 27-61.
- Hart, W. K., WoldeGabriel, G., Haile-Selassie, Y., and Renne, P. R., "Volcanic Record of the Adu-Asa Formation, pp. 63-91.
- Renne, P. R., Morgan, L. E., WoldeGabriel, G., and Hart, W. K., "Geochronology", pp. 93-103.